

Annual Review of Control, Robotics, and Autonomous Systems

Dynamic Walking: Toward Agile and Efficient Bipedal Robots

Jenna Reher¹ and Aaron D. Ames²

¹Department of Mechanical and Civil Engineering, California Institute of Technology, Pasadena, California 91125, USA; email: jreher@caltech.edu, ames@caltech.edu

Annu. Rev. Control Robot. Auton. Syst. 2021. 4:535–72

First published as a Review in Advance on December 11, 2020

The Annual Review of Control, Robotics, and Autonomous Systems is online at control.annualreviews.org

https://doi.org/10.1146/annurev-control-071020-045021

Copyright © 2021 by Annual Reviews. All rights reserved

ANNUAL CONNECT

www.annualreviews.org

- Download figures
- Navigate cited references
- Keyword search
- Explore related articles
- Share via email or social media

Keywords

robotics, control theory, optimization, hybrid systems, bipedal robots, dynamic walking

Abstract

Dynamic walking on bipedal robots has evolved from an idea in science fiction to a practical reality. This is due to continued progress in three key areas: a mathematical understanding of locomotion, the computational ability to encode this mathematics through optimization, and the hardware capable of realizing this understanding in practice. In this context, this review outlines the end-to-end process of methods that have proven effective in the literature for achieving dynamic walking on bipedal robots. We begin by introducing mathematical models of locomotion, from reduced-order models that capture essential walking behaviors to hybrid dynamical systems that encode the full-order continuous dynamics along with discrete foot-strike dynamics. These models form the basis for gait generation via (nonlinear) optimization problems. Finally, models and their generated gaits merge in the context of real-time control, wherein walking behaviors are translated to hardware. The concepts presented are illustrated throughout in simulation, and experimental instantiations on multiple walking platforms are highlighted to demonstrate the ability to realize dynamic walking on bipedal robots that is both agile and efficient.

²Control and Dynamical Systems Graduate Program, California Institute of Technology, Pasadena, California 91125, USA

1. INTRODUCTION

The realization of human-like capabilities on artificial machines has captured the imagination of humanity for centuries. The earliest attempts were made through purely mechanical means. In 1495, Leonardo da Vinci detailed his *Automa cavaliere*, a primitive humanoid in a knight's armor that was operated by pulleys and cables. However, these mechanical automatons lacked the ability to apply feedback control, and thus the field remained largely dormant until digital computers became broadly available. In 1921, 40 years before microprocessors were introduced, the word robot was coined by the Czech writer Karel Čapek, and soon thereafter the field of legged robots began to emerge.

Today, the field of robotic legged locomotion is of special interest to researchers, as humans increasingly look to augment their natural environments with intelligent machines. In order for these robots to navigate the unstructured environments of the world and perform tasks, they must have the capability to reliably and efficiently locomote. The first control paradigms for robotic walking used a notion of static stability, where the vertical projection of the center of mass (COM) is contained within the support polygon of the feet, leading to the WABOT 1 robot in the early 1970s at Waseda University (1) and the first active exoskeletons by Vukobratović at the Mihajlo Puppin Institute (2). This static stability criterion was very restrictive, leading to the development of the zero moment point (ZMP) criterion (3, 4), which enabled a wider range of robotic locomotion capabilities by generalizing from the COM to the center of pressure. Despite this generalization, the ZMP criterion still restricts the motion of the robot to be relatively conservative compared with the capabilities of biological walkers and does not allow for more dynamic motions (5). Nevertheless, this methodology has been perhaps the most popular methodology to date for realizing robotic locomotion and has been applied to various successful humanoid robots, such as the Honda ASIMO robot (6), the HRP series (7–9), and HUBO (10).

As the field progressed into the 1980s, it became clear that achieving truly dynamic locomotion would require further exploiting the natural nonlinear dynamics of these systems in a stable, energy-efficient fashion. In stark contrast to the concept of fully actuated humanoid locomotion, Marc Raibert and the MIT Leg Laboratory launched a series of hopping robots that demonstrated running behaviors and flips (11, 12). To achieve these behaviors, there was a shift from the conservative walking models encoded by the ZMP to reduced-order models [e.g., the spring-loaded inverted pendulum (SLIP)] that ensure dynamic locomotion through the creation of stable periodic orbits (13). Building on this core idea, Tad McGeer began development of completely passive walking machines, which would ultimately give rise to the field of passive dynamic walking (14). The downside of this method is that the system has little to no actuation with which it can respond to perturbations or perform other tasks. However, these breakthroughs were critical in demonstrating that dynamic robotic locomotion was possible on systems that were not fully actuated, and that this underactuation could actually be leveraged to improve their performance.

Despite the advances leading up to the turn of the century, there remained a growing gap between the physical capabilities of robotic systems and the development of controllers to exploit them. This was particularly stark in the area of underactuated walking, where the lack of formal approaches that leverage the intrinsically nonlinear dynamics of locomotion limited the ability to fully exploit the robot's actuation authority. In the early 2000s, a key contribution to this area was introduced by Jessy Grizzle and colleagues (15), in which they developed the notion of virtual constraints, or holonomic constraints enforced via control rather than a physical mechanism. Enforcing these constraints leads to low-dimensional invariant surfaces (zero dynamics surfaces) in the continuous phase of the model. These virtual constraints could then be designed such that this surface is hybrid invariant (invariant under both the continuous and discrete dynamics), ultimately

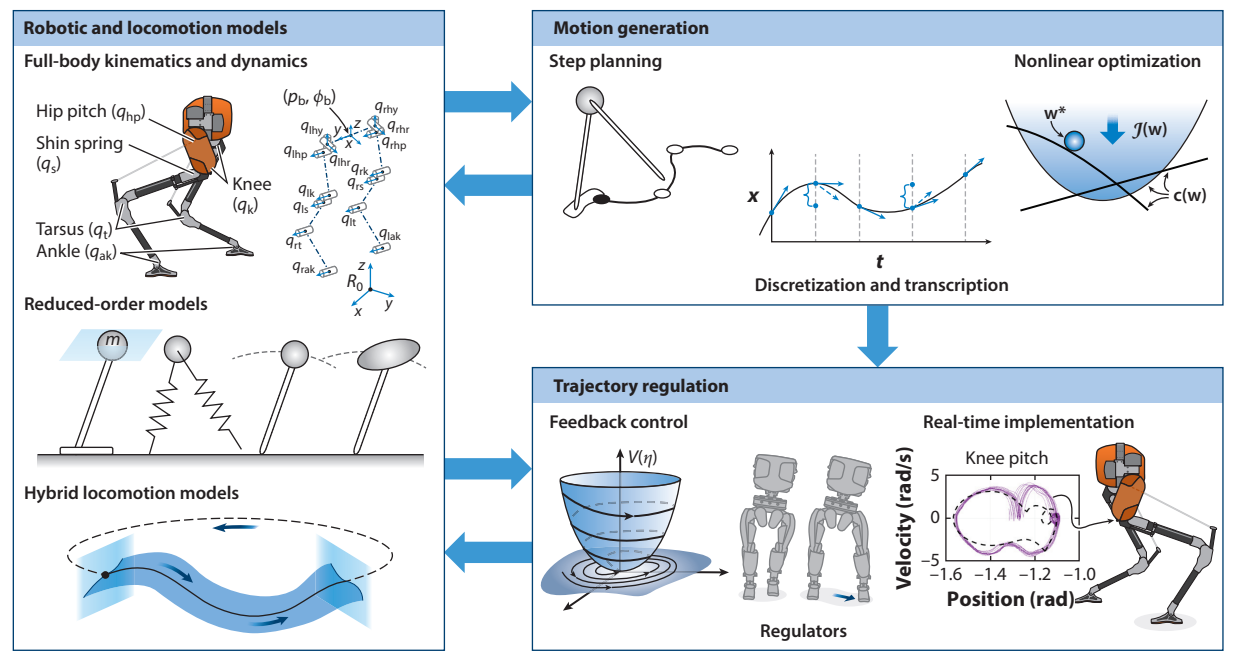


Figure 1

The interconnection of key components of dynamic walking. Dynamic walking is a complex behavior, requiring control designers and roboticists to simultaneously consider robotic models, the transcription of locomotion into a motion planning problem, and the coordination and actuation of the system via control laws. Some figure components adapted from Reference 21 with permission from Springer.

leading to the concept of hybrid zero dynamics (HZD) (16). The end result is formal guarantees on the generation and stabilization of periodic orbits (17), i.e., walking gaits. This paradigm for control of dynamic underactuated locomotion has pushed the boundaries of what is achievable, including fast running (18, 19) and efficient humanoid walking (20, 21).

As shown by this brief history of dynamic walking, each new methodology comes with a greater understanding of how to model, plan, and execute increasingly complex behaviors on these robotic systems. Due to the inherently difficult nature of dynamic walking, successes in the field have typically been achieved by considering all aspects of the problem, often with explicit consideration of the interplay between modeling and feedback control (see **Figure 1**). Specifically, the robotic and locomotive models that are used ultimately inform the planning problem and therefore the resulting behavior. Controllers that can actuate and coordinate the limbs must then be developed that, ideally, provide tracking, convergence, and stability guarantees. In this review, we therefore examine how this interplay among modeling, motion planning, and trajectory regulation has shaped dynamic walking on bipedal robots.

The remainder of this article is structured as follows. In Section 2, we present reduced-order models that have provided canonical examples of dynamic locomotion, and in Section 3, we introduce extensions to hybrid system models for dynamic walking. Section 4 discusses how these models have been used to generate stable walking motions through various motion planning approaches and corresponding optimization problems. Finally, Section 5 provides several existing methods for controlling a robot, as informed by the methods introduced in the earlier sections,

with a view toward hardware realization. This interconnection can be seen in **Figure 1**, where each section is informed by the prior one.

2. DYNAMIC MODELS OF BIPEDAL LOCOMOTION

In this section, we provide background on the modeling of dynamic bipedal robots and contextualize several of the most popular approaches for encoding or approximating locomotion via reduced-order models. A unifying theme among the broad spectrum of models used for legged locomotion, in both this section and the next, is that the system must undergo intermittent contact with the surrounding environment in order to move. This fact is inextricably tied to legged locomotion. How the overall walking system is ultimately modeled plays a critical role in the planning and control approaches that realize locomotion.

2.1. Bipedal Robots: Floating-Base Systems with Contacts

Bipedal robotic platforms are conveniently modeled using a tree-like structure with an ordered collection of rigid linkages. This structure lends itself well to generalization, and tools to facilitate the generation of symbolic (22) or algebraic (23) expressions for the kinematics and dynamics of the robot are therefore commonly used. The robot itself must ambulate through a sequence of contact conditions with the environment. Because interactions with the environment are always changing, a convenient method for modeling the system is to construct a representation of the robot in a general position, and then enforce ground contacts through forces arising from the associated holonomic constraints that are imposed at the feet. This is often referred to as the floating-base model of the robot.

2.1.1. The configuration space. To represent the floating base, let R_0 be a fixed inertial frame attached to the world and let R_b be a body reference frame rigidly attached to the pelvis of the robot with the origin located at the center of the hip. Then the Cartesian position $p_b \in \mathbb{R}^3$ and orientation $\psi_b \in SO(3)$ compose the floating-base coordinates of frame R_b with respect to R_0 . The remaining coordinates that dictate the shape of the actual robot, $q_1 \in \mathcal{Q}_1 \subset \mathbb{R}^{n_1}$, are the local coordinates representing rotational joint angles and prismatic joint displacements. **Figure 2***a* shows an image of this floating-base coordinate system definition for a Cassie bipedal robot. The combined set of coordinates is $q = (p_b^T, \phi_b^T, q_1)^T \in \mathcal{Q} = \mathbb{R}^3 \times SO(3) \times \mathcal{Q}_1$ with the states $x = (q^T, \dot{q}^T)^T \in T\mathcal{Q} = X$.

2.1.2. Continuous dynamics. Traditional methods for modeling the dynamics of floating-base systems typically result in the separation of the equations of motion into multiple parts (24)—one arising from the multibody continuous dynamics, and the other imposed via constraints on contacts with the environment. If we continue with the assumption that the robot structure is a rigid collection of linkages, then we can consider the continuous dynamics of a bipedal robot in the Lagrangian form (see 25):

$$D(q)\ddot{q} + H(q, \dot{q}) = Bu + J_{h}(q)^{T}\lambda,$$
1.

where D(q) is the inertia matrix, $H(q, \dot{q})$ contains the Coriolis and gravity terms, B is the actuation matrix, $u \in U \subseteq \mathbb{R}^m$ is the control input, and the Jacobian of the holonomic constraints applied to the robot is $J_h(q) = \frac{\partial b}{\partial q}(q)$, with the corresponding wrenches $\lambda \in \mathbb{R}^{m_h}$. These dynamics can be

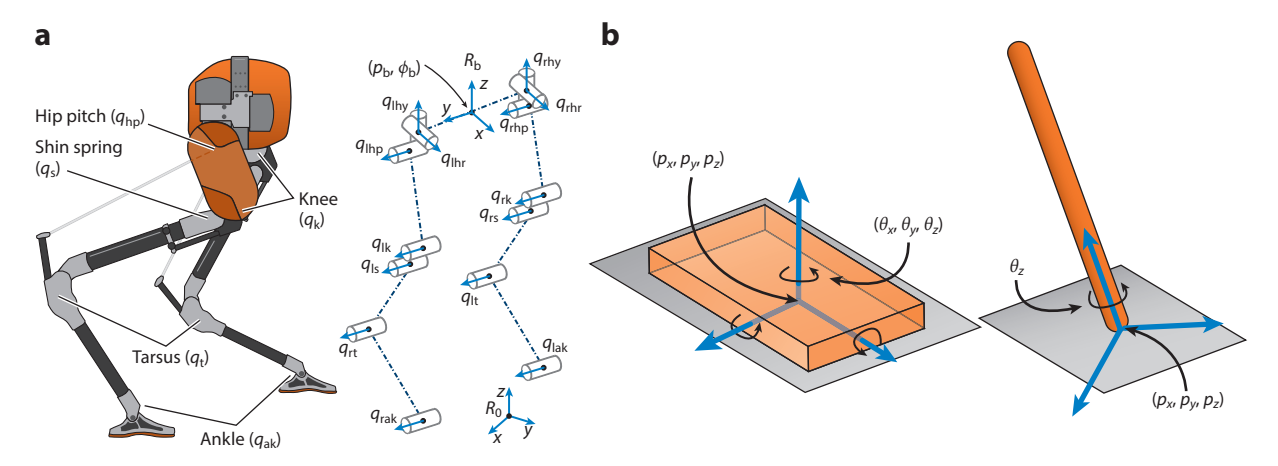


Figure 2

A visual demonstration of the robotic configuration and contact constraints that are applied to the robot. (a) The floating-base coordinate system for a Cassie bipedal robot, with a coordinate frame attached to the hip and rotational joints connecting rigid linkages of the body. (b) The contact geometry of the constraints for an underactuated flat-foot contact and a point-foot contact.

expressed in a state-space representation as

$$\frac{\mathrm{d}}{\mathrm{d}t} \begin{bmatrix} q \\ \dot{q} \end{bmatrix} = \underbrace{\begin{bmatrix} \dot{q} \\ D^{-1}(q) \left(J_{h}(q)^{\mathrm{T}} \lambda - H(q, \dot{q}) \right) \end{bmatrix}}_{f(x)} + \underbrace{\begin{bmatrix} 0 \\ D(q)^{-1} B \end{bmatrix}}_{g(x)} u.$$
 2.

2.1.3. Contact forces. The fact that the robotic model is derived using a floating-base representation means that as we manipulate the robot, the resulting ground force interaction through the Lagrangian dynamics in Equation 1 is critical. The most popular method for modeling ground interaction is to assume rigid contacts with nonpenetration; the resulting forces are then considered unilateral (24), meaning that they can push but not pull on the ground. The resulting normal force cannot be negative, $\lambda_z \geq 0$, and this implies that when this condition crosses zero, the contact will leave the ground. A point of the robot in static contact with the ground will satisfy a closure equation of the form

$$\eta(q) = \begin{bmatrix} p_{c}(q)^{\mathrm{T}}, & \phi_{c}(q)^{\mathrm{T}} \end{bmatrix}^{\mathrm{T}} = \text{constant},$$
3.

where $p_c(q)$ is the Cartesian position of the contact point and $\phi_c(q)$ is a rotation between contacting bodies (26). Differentiating twice yields acceleration constraints on the robot,

$$J_{\rm h}(q)\ddot{q} + \dot{J}_{\rm h}(q,\dot{q})\dot{q} = 0, \tag{4}$$

leading to a system of equations, with Equations 1 and 4 coupling the accelerations to the inputs and resulting constraint forces. The geometry of robotic feet is often given as either a flat foot or a single point of contact, as shown in **Figure 2***b*. Assuming three noncollinear points of contact, the foot can be modeled as a flat plane. The position and orientation of the plane with respect to the ground will then create a six-degree-of-freedom closure constraint in Equation 3 ($m_h = 6$). Alternatively, many underactuated robots have point feet. If the assumption is made that the foot will not yaw while in contact, then this will form a four-degree-of-freedom constraint on the Cartesian positions and rotation about the z axis ($m_h = 4$).

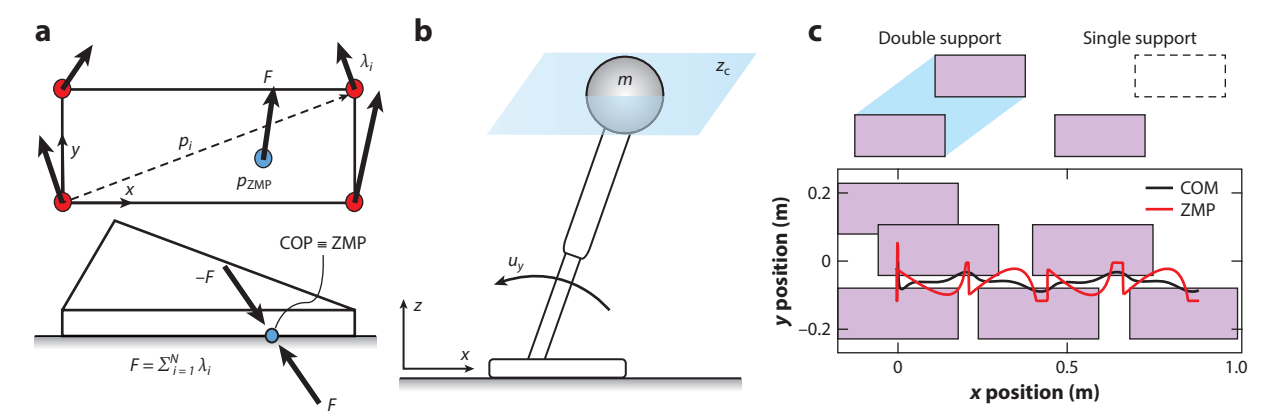


Figure 3

The principles and modeling assumptions of the LIPM approach. (a) Visualization of the ZMP, where the foot is dynamically balanced if the resultant force F is within the support polygon. (b) LIPM with a telescoping leg and actuated ankle to control the robot along a horizontal surface. (c) Support polygon and an example of a planned ZMP trajectory. Abbreviations: COM, center of mass; COP, center of pressure; LIPM, linear inverted pendulum model; ZMP, zero moment point.

Finally, when designing motions for the robot, it is important to also model the real-world limitations on the allowed tangential force before it will break a nonslip condition. The most popular approach is to employ a classical Amontons–Coulomb model of (dry) friction (26). For a friction coefficient μ , the space of valid reaction forces is characterized by the friction cone:

$$C = \left\{ (\lambda_x, \lambda_y, \lambda_z) \in \mathbb{R}^3 \middle| \lambda_z \ge 0; \sqrt{\lambda_x^2 + \lambda_y^2} \le \mu \lambda_z \right\}.$$
 5.

2.2. Linear Inverted Pendulums and the Zero Moment Point

In this section, we describe the basic aspects of the ZMP and how it has been used in linear inverted pendulum models (LIPMs) of locomotion. The concept of the ZMP is identical to the center of pressure and was originally introduced through a series of observations on the stability of anthropomorphic walkers by Vukobratović and colleagues (3, 27) in the early 1970s. The primary interpretation of the ZMP is that it represents the point on the ground at which the reaction forces between the robot's contacts and the ground produce no horizontal moment. Consider a robot standing in single support, with a finite number of contact points (p_i) that constrain the foot to be flat. As shown in **Figure 3**a, the resultant forces will consist of normal (λ_n) and tangential (λ_t) components. The ZMP is then computed as

$$p_{\text{ZMP}} := \frac{\sum_{i=1}^{N} p_i \lambda_{i,n}}{\sum_{i=1}^{N} \lambda_{i,n}}.$$
6.

This led to perhaps the most commonly used dynamic stability margin (28–32), referred to as the ZMP criterion, which states that a movement is stable so long as the ZMP remains within the convex hull of the contact points (also known as the support polygon). This notion is conservative, and controlling these motions typically requires the robot to remain fully actuated, with position-controlled joints and load cells in the feet.

The ZMP criterion has been tied extensively to the LIPM in order to considerably simplify the trajectory design process, as the ZMP can be written explicitly in terms of the COM dynamics (33). This has led many researchers to consider a Newton–Euler representation of the centroidal

dynamics, written as

$$m(\ddot{c}+g) = \sum_{i} \lambda_{i}, \qquad \dot{L} = \sum_{i} (p_{i}-c) \times \lambda_{i},$$
 7.

where c is the COM position; $L = \sum_k (x_k - c) \times m_k \dot{x}_k + \mathbf{I}_k \omega_k$ is the angular momentum; g is the gravitational acceleration; λ_i is the contact forces; p_i is each contact force position; \dot{x}_k and ω_k are the linear and angular velocities on the kth linkage, respectively; m_k and \mathbf{I}_k are the masses and inertia tensors, respectively; and m is the total mass of the robot.

If we constrain the motion of a fully actuated inverted pendulum with a massless telescoping leg such that the COM moves along a horizontal (x,y) plane, then we obtain a linear expression for the robot dynamics. An example of the LIPM is visualized in **Figure 3***b*. The dynamics of the LIPM at a given height, z_c , is

$$\ddot{x} = \frac{g}{z_c} x + \frac{1}{mz_c} u_y, \qquad \ddot{y} = \frac{g}{z_c} y + \frac{1}{mz_c} u_x,$$
 8.

where m is the mass of the robot, g is the acceleration of gravity, and u_x and u_y are the torques about the x and y axes, respectively, of the attachment to the ground (i.e., the ankle). The ZMP location on the ground can also be directly written in terms of the LIPM dynamics as

$$p_{\rm ZMP}^{x} = x - \frac{z_{\rm c}}{g}\ddot{x}, \qquad p_{\rm ZMP}^{y} = y - \frac{z_{\rm c}}{g}\ddot{y}.$$
 9.

The LIPM can be viewed as a cart—table system (4), where the cart—table lies on a base with a geometry corresponding the support polygon (34). Designing walking with the ZMP can be essentially reduced to an inverse kinematics problem, where the primary planning is done on the ZMP trajectory. **Figure 3**c shows an example ZMP trajectory for several forward steps, where the trajectory for this walking is planned so that the ZMP always stays within the support polygon. ZMP walking has been applied largely to humanoids, such as the WABIAN robots (1), the HRP series (7, 9), Johnnie (35), and HUBO (10).

2.3. Capturability and Nonlinear Inverted Pendulum Models

Rather than characterize the stability of walking based on the ZMP, Pratt et al. (36) and Hof (37) independently introduced the idea of a capture point, referred to by Hof as the extrapolated center of mass. The capture point can be intuitively described as the point on the ground onto which the robot has to step to come to a complete rest. In canonical examples of the capture-point methods, the overall walking motions of the robot are planned and controlled based on the (instantaneous) capture-point dynamics. In this case, the COM of the robot is constrained to move at a constant height along a horizontal plane and thus uses a linear inverted pendulum representation of the robotic system. Koolen et al. (38) showed that for the compound variable $r_{\rm ic}^{x,y} = c + \sqrt{\frac{z_c}{g_c}} \dot{c}$, the unstable portion of the resulting system dynamics (along the horizontal direction) can be written in a constrained fashion as

$$\dot{r}_{\mathrm{ic}}^{x,y} = \sqrt{\frac{g_z}{z_{\mathrm{c}}}} (r_{\mathrm{ic}}^{x,y} - r_{\mathrm{CMP}}^{x,y}), \quad \text{subject to} \quad r_{\mathrm{ic}}^{x,y} \in \mathrm{conv}\{p_i^{x,y}\}, \quad 10.$$

where $r_{ic}^{x,y}$ is the horizontal location of the instantaneous capture point. The main consideration of the locomotion process is then to ensure that feet are placed such that $r_{ic}^{x,y}$ lies within the support polygon. Satisfying this condition means that the COM will converge to the capture point and come to a rest.

Despite this intuitive representation of stability, the LIPM walking simplifications come with a steep cost due to the stringent requirements on the motion and actuation of the robot. Yet

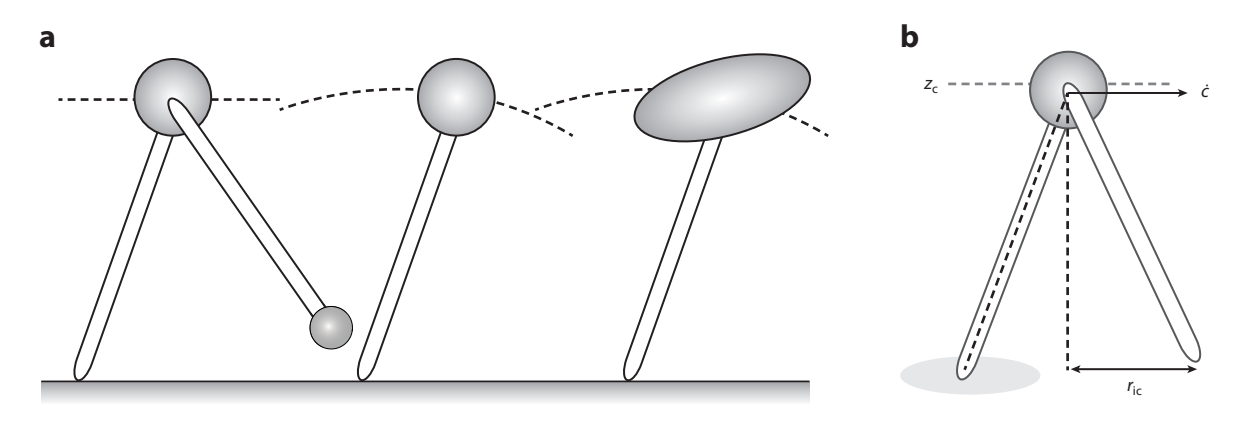


Figure 4

(a) Several variations on inverted pendulum models, which attempt to expand the possible behaviors of the robot by accounting for more of the body inertia or by releasing the constrained motion of the hip. (b) The capture point for a linear inverted pendulum walking robot.

it is precisely these characteristics that make the model most suitable for performing complex, multi-objective tasks that include manipulation during intermittent conservative motions. The maturity and reliability of the LIPM made it prevalent in the walking controllers used at the DARPA Robotics Challenge (39–41).

In an attempt to overcome issues associated with the strict assumptions of the LIPM, researchers have introduced more complex pendulum models (illustrated in **Figure 4***a*). The largest constraint on LIPM walking is the assumption of constant COM height, leading to the development of a nonlinear inverted pendulum with a variable mass height (42). To account for the inertia of a swinging leg, Park & Kim (43) proposed the addition of a mass at the swing foot, which they termed the gravity-compensated LIPM. One of the most commonly used models in the literature to address nontrivial angular momenta from the limbs of large robots moving dynamically is to add a flywheel to the hip, which can be used to represent the inertia of the robot body as it moves (44). A flywheel model of the robot has gained recognition as a convenient representation of the robotic system, particularly for capture-point control (36, 45). Various pendulum models have been widely used in analysis of push recovery and balance (46–49). The capture-point approach has also been used to demonstrate walking successfully on hardware (38, 50) and was famously used on Honda's ASIMO (51, 52).

2.4. The Spring-Loaded Inverted Pendulum

Classic work by Raibert and colleagues on hopping and running robots in the 1980s demonstrated the efficacy of using compliant models in locomotion through the development of a planar hopper that could bound at a speed of 1 m/s (11) and a 3D hopper that could achieve running without a planarizing boom (12). These early successes drove researchers to investigate a SLIP representation of bipedal robots (shown in **Figure 5***a*). The SLIP model provides a low-dimensional representation of locomotion that draws inspiration from biological studies of animal locomotion (53, 54). The SLIP is particularly attractive due to its inherent efficiency and robustness to ground height variations.

To use this model to synthesize controllers for actual robots, the control objectives are typically decomposed into three components: achieving a particular foot-strike location to regulate forward

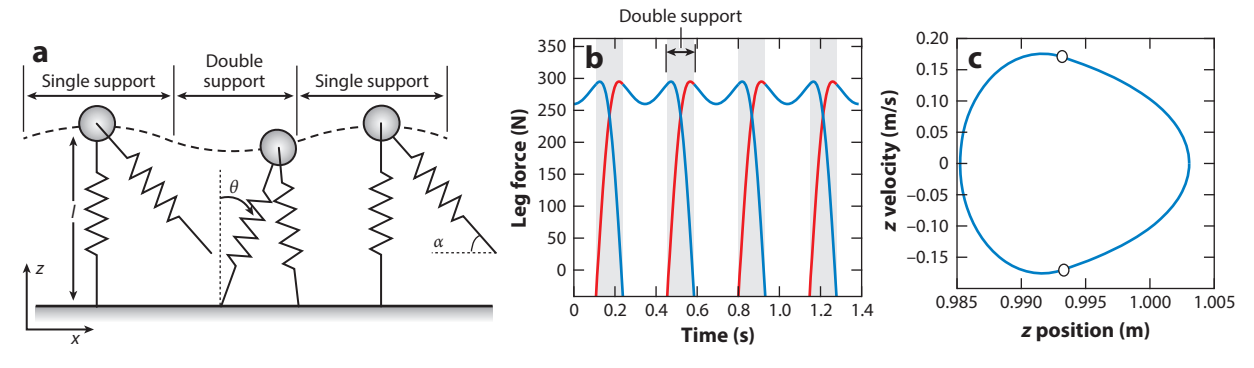


Figure 5

(a) The SLIP model, with the mass at the hip and virtual compliant legs. (b) Contact forces during walking, where the double-hump profile is observed in biological walkers. (c) A periodic orbit for the vertical COM coordinate, where a lack of impact yields no foot-strike discontinuity. Abbreviations: COM, center of mass; SLIP, spring-loaded inverted pendulum.

speed, injecting energy through either passive compliance or motors to regulate the vertical height of the COM, and regulating the posture of the robot. One then designs the walking and running motions with SLIP models and compensates for model mismatch or disturbances with well-tuned foot-placement-style controllers (55–59) (see Section 5.2). To this end, the dynamics of the SLIP are derived by assuming that the mass of the robot is concentrated at the hip with virtual springy legs:

$$0 = m\ddot{l} - ml\dot{\theta}^2 + mg\sin(\theta) + F_{\text{slip}},$$

$$0 = m[l^2\ddot{\theta} + 2l\dot{l}\dot{\theta}] + mgl\sin(\theta),$$
11.

where l is the stance leg length, θ is the stance leg angle, and $F_{\rm slip}$ is the force arising from the spring compression. One of the signature characteristics of this model is the double-hump profile of the reaction forces (shown in **Figure 5b**), which is described by the force interactions observed in biological walkers (54). A key contribution introduced by the SLIP community is the handling of underactuated behaviors, with many of the corresponding robots having point-feet and flight phases of motion. Finding a stable gait thereon does not rely on the quasi-static assumptions used for the fully actuated pendulum walkers of the preceding sections, instead focusing on stable cyclic locomotion. Dynamic stability is defined based on a constraint on the periodicity of the walking (detailed in the sidebar titled Periodic Notions of Stability). To achieve forward walking, the initial states of the robot and the angle of attack α for the swing leg are chosen to yield a periodic gait (see **Figure 5c**). It is important to note that since the legs are massless, impacts are not considered, and the resulting orbit will be closed with no instantaneous jumps in the velocity.

The SLIP representation of walking has been used primarily for legged robots that have springs or series-elastic actuators. Some of the earliest inclusions of compliant hardware on bipedal robots were with a spring flamingo and spring turkey (64). Later, the COMAN robot included passive compliance to reduce energy consumption during walking (65), and the Valkyrie robot from NASA was the first full-scale humanoid robot to heavily use series-elastic actuators (66). Using inspiration from the SLIP morphology, Hurst and colleagues designed the planar humanoid robot MABEL (67) and the 3D bipedal robot ATRIAS (68, 69) to include series-elastic actuation and thus return energy through impacts and shield the motors from impact forces at foot strike. One of the latest robots in this series, the Cassie biped (shown in **Figure 2a**), also mechanically approximates SLIP design principles (70). Several running robots have specifically considered SLIP model

PERIODIC NOTIONS OF STABILITY

One can view steady-state walking as a periodic motion that is not instantaneously stable but is stable from foot strike to foot strike (60)—in other words, walking is controlled falling. Concretely, a solution $\phi(t, t_0, x_0)$ to a dynamical system $\dot{x} = f(x)$ is periodic if there exists a finite T > 0 such that $\phi(t + T, t_0, x_0) = \phi(t, t_0, x_0)$ for all $t \in [t_0, \infty)$, and a set $\mathcal{O} \subset X$ is a periodic orbit if $\mathcal{O} = \{\phi(t, t_0, x_0) | t \ge t_0\}$ for some periodic solution $\phi(t, t_0, x_0)$. In a seminal paper on passive dynamic walking, McGeer (14) popularized the method of Poincarè to determine the existence and stability of periodic orbits (61) for walking. In this approach, one step is considered to be a mapping from the walker's state x_k at a definite point within the motion of a stride (typically defined at foot strike) to the walker's configuration at the same point in the next step, x_{k+1} . Let \mathcal{S} define the Poincarè section, for which we have a Poincarè map $P: \mathcal{S} \to \mathcal{S}$ that maps one step to the next as $x_{k+1} = P(x_k)$. The periodic orbit yields a fixed point $x^* = P(x^*)$ with $x^* \in \mathcal{O} \cap \mathcal{S}$, and the stability of the orbit is equivalent to the stability of the Poincarè map, which can be checked numerically (62, 63).

principles in their mechanical design, such as the ARL Monopod II (71), Carnegie Mellon University's Bowleg Hopper (72), and the Keneken hopper (73).

3. HYBRID SYSTEM MODELS OF BIPEDAL LOCOMOTION

In the drive to obtain efficient legged locomotion and understand the stability thereof, researchers have adopted more dynamic paradigms for robotic locomotion that consider nontrivial impacts and periodic notions of stability. To formalize this perspective, it is necessary to consider hybrid system models of walking, which include both continuous (leg swing) and discrete (foot strike) dynamics. This section discusses two key paradigms that leverage this framework: passive dynamic walking, which exploits the natural hybrid dynamics of the system to obtain efficient walking, and HZD, which uses actuation to achieve model reduction and thereby synthesize stable walking gaits.

3.1. Passive Dynamic Walking

Some of the first work to study hybrid systems for the purposes of synthesizing walking were within the field of passive dynamic walking. McGeer (14, 74) introduced several passive walking robots that could ambulate down small declines when started from a reasonable initial condition. While these early bipeds were completely passive and relied on gravity, several bipeds were built to demonstrate that simple actuators could substitute for gravitational power and compensate for disturbances. Small electric actuators were used for the Cornell walkers (75–77) and the MIT learning biped (78, 79), while the Delft biped instead used a pneumatic actuator at the hip (80, 81). Controlled symmetries (82) and geometric reduction (83) have been used to extend these ideas to actuated robots and 3D walking. Actuated environments have also been used to excite walking on passive robots (84). Because of the care taken in mechanical design, these robots could all operate without sophisticated real-time calculations—though at the cost of diminished control authority.

The governing equations of motion for passive dynamic robots are nonlinear and correspond to the continuous dynamics derived in Equation 1 rather than using an approximate (or reduced-order) model. They are also hybrid, meaning they consist of both continuous and discrete nonlinear dynamics. A definition of the hybrid representation of the dynamics of walking is summarized in the sidebar titled Hybrid Dynamical Systems, where the key element that determines the behavior is a directed cycle of continuous domains.

HYBRID DYNAMICAL SYSTEMS

A hybrid dynamical system, which is used to model a walking robot (85), is defined as the tuple

$$\mathcal{H} = (\Gamma, \mathcal{D}, S, \Delta, F),$$

where the variables are as follows:

- $\Gamma = \{V, E\}$ is a directed cycle specific to the desired walking behavior, with V the set of vertices and E the set of edges, $e = (v_s \to v_t) \in E$ with $v_s, v_t \in V$, in the cycle.
- $\mathcal{D} = \{\mathcal{D}_v\}_{v \in V}$ is the set of domains of admissibility. Each domain \mathcal{D}_v can be interpreted as the set of physically realistic states of the robot.
- $S = \{S_{\varepsilon}\}_{\varepsilon \in E}$ is the set of guards, with $S_{\varepsilon} \subset \mathcal{D}_{v_s}$, that form the transition points from one domain, \mathcal{D}_{v_s} , to the next in the cycle, \mathcal{D}_{v_r} .
- $\Delta = \{\Delta_{e}\}_{e \in E}$ is the set of reset maps, $\Delta_{e} : S_{e} \subset \mathcal{D}_{v_{s}} \to \mathcal{D}_{v_{t}}$, from one domain to the next. The reset map gives the postimpact state of the robot: $x^{+} = \Delta_{e}(x^{-})$.
- $F = \{f_v\}_{v \in V}$ is a set of dynamical systems where $\dot{x} = f_v(x)$ for coordinates $x \in D_v$, i.e., of the form given in Equation 2 with u = 0.

3.1.1. Discrete dynamics: impacts and Poincarè maps. An inherent feature of dynamic walking is that the robot is moving quickly through the environment. Thus, the resulting motions cannot be slow enough for the feet to approach the ground with negligible velocity, and impacts with the ground become an important consideration. Formally accounting for impacts underlies the basis for hybrid dynamical locomotion models (16, 26, 85). Impacts during walking occur when the nonstance foot strikes the ground. Concretely, consider the vertical distance (height) of a contact point (foot) above the ground, $H_{\epsilon}(x)$. Impacts occur when the system reaches the switching surface of the guard:

$$S_e = \{x \in X \mid H_e(x) = 0, \dot{H}_e(x) < 0\},$$
 12.

where this surface is also a Poincarè section that will be used to construct the Poincarè map. At each transition, the new initial condition is determined through the reset map:

$$\begin{bmatrix} q^+ \\ \dot{q}^+ \end{bmatrix} = \begin{bmatrix} \mathcal{R}q^- \\ \mathcal{R}\Delta_{\dot{q}}(q^-)\dot{q}^- \end{bmatrix} = \Delta(q^-, \dot{q}^-),$$
 13.

where \mathcal{R} is a relabeling matrix (16, 86), which flips the stance and nonstance legs. Here, Δ_q describes the change in velocity that occurs at impact and is typically calculated using the assumption of a perfectly plastic impact (87, 88). Note that determining and utilizing more complex impact models is an open problem. In real life, impacts are not truly instantaneous and do not always achieve stiction (89). Situations with multiple impacts can arise (90), leading to Zeno behaviors (91–93) or slippage (94, 95).

A canonical example of passive dynamic walking is an unactuated compass biped walking down a slope of angle γ (96) (see **Figure 6a**). This robot consists of two kneeless legs, each with a point mass, and a third mass at the hip. The directed cycle for the biped consists only of a single-support domain, with transition occurring at foot strike (shown in **Figure 6b**). The periodic nature of the stable walking behavior is best summarized by the phase portrait in **Figure 6c**, where there are discrete jumps occurring at impact. The stability of a cyclic gait is discussed in the sidebar titled Periodic Notions of Stability. Once a fixed point x^* has been found, we can examine a first-order

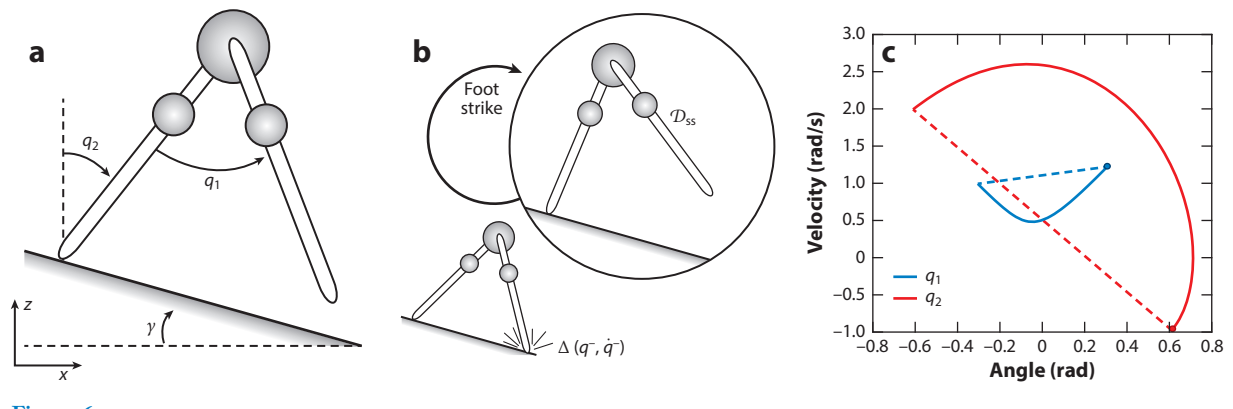


Figure 6

A canonical example of passive dynamic walking: the compass biped. (a) The biped and its configuration on the slope. (b) A directed graph of the corresponding hybrid dynamical system. (c) A closed limit cycle for the biped walking down a 5° slope, implying stable walking.

expansion of the Poincarè map:

$$P(x^* + \delta x) \approx x^* + \frac{\partial P}{\partial x}(x^*)\delta x$$
, with $P(x^*) = x^*$, $x^* \in \mathcal{O} \cap S_c$, 14.

where the fixed point is exponentially stable if the magnitude of the eigenvalues of $\frac{\partial P}{\partial x}(x^*)$ is less than one (61–63). This is straightforward to check numerically: One can construct a numerical approximation of successive rows by applying small perturbations to each corresponding state and then forward simulate one step to obtain $P(x^* + \delta x)$.

3.2. Hybrid Zero Dynamics

The HZD method leverages nonlinear feedback control design to induce stable locomotion on underactuated robots. Grizzle and colleagues (15, 97, 98) introduced the concept and developed a set of tools that are grounded in nonlinear control theory to deal formally with the nonlinear and hybrid nature of dynamic walking [see the textbook by Westervelt et al. (16)]. The basis of the HZD approach is the restriction of the full-order dynamics of the robot to a lower-dimensional attractive and invariant subset of its state space, the zero dynamics surface, via outputs that characterize this surface. If these outputs are driven to zero, then the closed-loop dynamics of the robot are described by a lower-dimensional dynamical system that can be shaped to obtain stability.

As was the case for uncontrolled hybrid models generalizing hybrid dynamical systems, a hybrid control system (see the sidebar titled Hybrid Control Systems) describes an actuated walking robot, leading to the notion of HZD. The primary consideration that governs the overall locomotion problem is the specification of a directed cycle for the underlying hybrid (control) system. Because HZD incorporates feedback control, significantly more complex motions are possible. Figure 7 shows examples of directed cycles for dynamic walking behaviors, illustrating how domain specification is governed largely by the evolution of the contacts through the course of a step. Figure 8 presents the controlled compass walker (96) to provide a comparison with passive dynamic walking. In this example, torques applied at the hip are used to control the motion, while the robot walks with a stable limit cycle on flat ground.

HYBRID CONTROL SYSTEMS

Rather than describing a passive hybrid system (as in the Hybrid Dynamical Systems sidebar), the incorporation of a feedback control allows for the realization of more advanced behaviors on complex actuated bipedal robots. We therefore define a hybrid control system (85, 99) to be the tuple

$$\mathcal{HC} = (\Gamma, \mathcal{D}, \mathcal{U}, S, \Delta, FG),$$

where the variables are as follows:

- \blacksquare Γ , \mathcal{D} , S, and Δ are defined as in the Hybrid Dynamical Systems sidebar.
- $\mathcal{U} = \{\mathcal{U}_v\}_{v \in V}$ is the set of admissible control inputs.
- $FG = (f_v, g_v)_{v \in V}$ is the set of control systems, $\dot{x} = f_v(x) + g_v(x)u$, as in Equation 2.

3.2.1. Virtual constraints and stabilization. Dynamic walking that leverages the full-body dynamics must necessarily include specifications on how the robot should coordinate its limbs in a holistic fashion. To this end, and analogous to holonomic constraints, virtual constraints are defined as a set of functions that regulate the motion of the robot to achieve a desired behavior (16). The term virtual comes from the fact that these constraints are enforced through feedback controllers instead of through physical constraints. Let $y^a(q)$ be functions of the generalized coordinates that are to be controlled (i.e., encoding the actual behavior of the robot) and $y^d(t, \alpha)$ be the desired behavior, where α is a matrix of real coefficients that parameterize this behavior. A Bézier polynomial is the most typical choice of representation for the desired outputs (16) for computational reasons, though humans appear to follow a spring-mass-damper-type behavior (86). Given actual y^a and desired y^d outputs, a virtual constraint is their difference:

$$\gamma(q) := \gamma^{\mathbf{a}}(q) - \gamma^{\mathbf{d}}(\tau(q), \alpha), \tag{15}$$

where $\tau(q): \mathcal{Q} \to \mathbb{R}$ is a parameterization of time that is strictly increasing along periodic motions. Driving $y \to 0$ results in convergence of the actual outputs to the desired outputs.

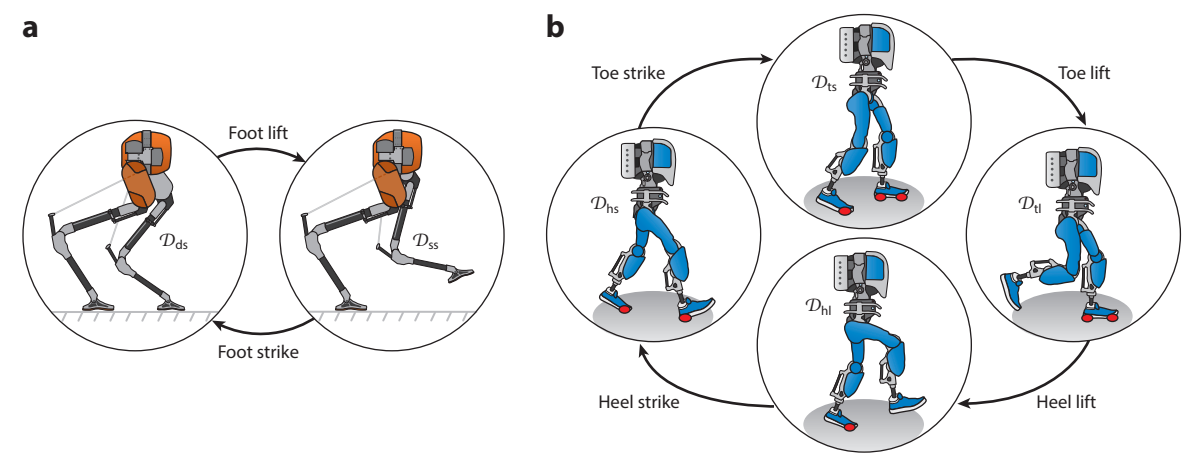


Figure 7

Examples of directed cycles for hybrid representations of (a) two-domain walking with compliance and (b) four-domain human-like robotic walking. Panel a adapted from Reference 100 with permission from IEEE.

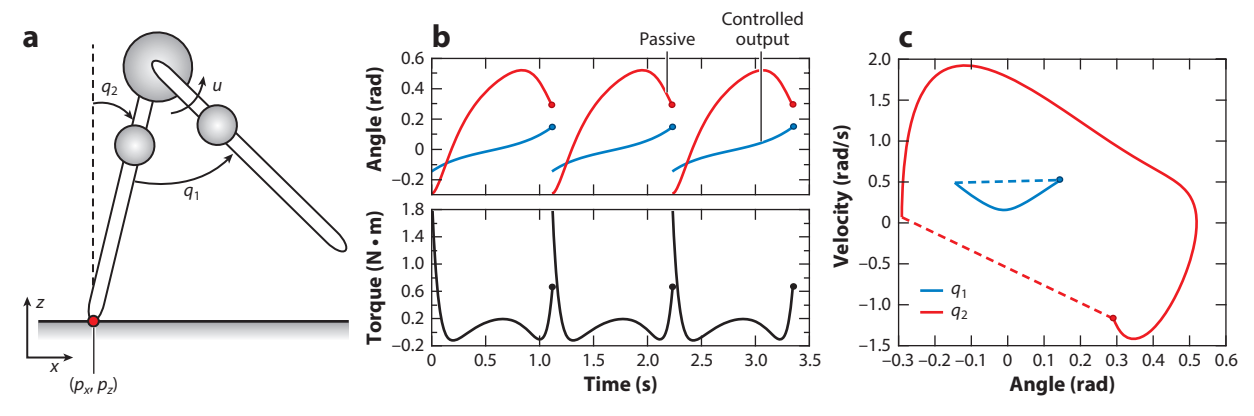


Figure 8

An example of HZD-based control for a compass biped on flat ground. (a) The robotic configuration. (b) Joint trajectories and torques over three steps of stable walking, (c) A stable limit cycle during the walking, with discrete jumps occurring at impact. Abbreviation: HZD, hybrid zero dynamics.

> To synthesize controllers, note that differentiating y(q) along solutions to the control system in Equation 2 yields the Lie derivatives:

$$\dot{y}(q,\dot{q}) = L_f y(q,\dot{q}), \qquad \ddot{y}(q,\dot{q}) = L_f^2 y_2(q,\dot{q}) + L_g L_f y(q,\dot{q})u,$$
 16.

where y(q) has vector relative degree 2 (101) if the matrix $L_g L_f y(q, \dot{q})$ is invertible. From this, one obtains the following feedback linearizing controller:

$$u^*(x) = \left[L_g L_f y(x)\right]^{-1} \left(-L_f^2 y(x) + \mu\right) \qquad \Rightarrow \qquad \ddot{y}(q, \dot{q}) = \mu, \tag{17}.$$

where μ is the auxiliary feedback component of the controller that can be chosen to stabilize the system. In particular, one common choice is $\mu = \frac{1}{\epsilon^2} K_p y(x) + \frac{1}{\epsilon} K_d L_f y(x)$, with K_p and K_d feedback gains chosen so that the linear dynamics are stable, and $\epsilon > 0$ a parameter used to amplify convergence to the desired motion, rendering the output dynamics exponentially stable. Applying Equation 17 with μ results in the closed-loop system

$$\dot{x} = f_{cl}(x) = f(x) + g(x)u^*(x),$$
 18.

where for this system $y \to 0$ exponentially fast.

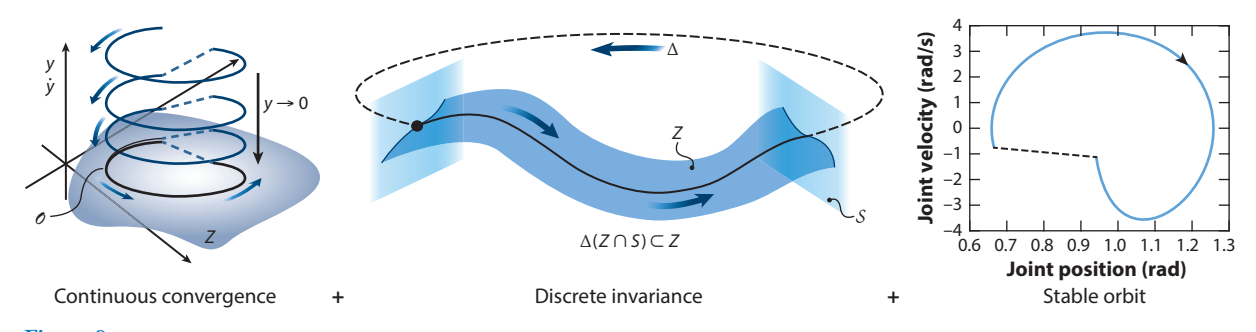
3.2.2. Hybrid invariance. The feedback control law of Equation 17 can be synthesized for virtual constraints $y_v(q) = y_v^a(q) - y_v^d(\tau(q,t),\alpha_v)$ associated with each domain $\mathcal{D}_v, v \in V$, and control system: $\dot{x} = f_v(x) + g_v(x)u$. This renders the zero dynamics manifold (102),

$$\mathbb{Z}_{v} = \{ (q, \dot{q}) \in \mathcal{D}_{v} \mid y_{v}(q) = 0, \, \dot{y}_{v}(q, \dot{q}) = 0 \},$$
19.

forward invariant and attractive. Thus, the continuous dynamics in Equation 18 will evolve on \mathbb{Z}_n given an initial condition in this surface. However, because the surface in Equation 19 has been designed without taking into account the hybrid transition maps of Equation 13, the resulting walking cycle may not be invariant to impact. To enforce impact invariance, the desired outputs can be shaped through the parameters α_v in γ_v^d such that the walking satisfies the HZD condition

$$\Delta_{e}(\mathbb{Z}_{v_{s}} \cap S_{v_{s}}) \subset \mathbb{Z}_{v_{t}}, \qquad \forall e = (v_{s}, v_{t}) \in E,$$
 20.

imposed as a constraint on the states through impact (Equation 13).



Key concepts related to HZD: continuous convergence to a zero dynamics surface Z, coupled with a hybrid invariance condition $\Delta(Z \cap S) \subset Z$, to obtain stable periodic walking. Abbreviation: HZD, hybrid zero dynamics.

The overarching goal of these constructions is to provide a framework for the synthesis of dynamic walking gaits. In this context, for simplicity (and without loss of generality) assume a single domain $V = \{v\}$, wherein we will drop the subscript v. For the full-order dynamics, let $\phi_t^{f_{\rm cl}}(x_0)$ be the (unique) solution at time $t \geq 0$ with initial condition x_0 . For a point $x^* \in S$, we say that $\phi_t^{f_{\rm cl}}$ is hybrid periodic if there exists a T > 0 such that $\phi_T^{f_{\rm cl}}(\Delta(x^*)) = x^*$. Furthermore, the stability of the resulting hybrid periodic orbit, $\mathcal{O} = \{\phi_t^{f_{\rm cl}}(\Delta(x^*)) : 0 \leq t \leq T\}$, can be found by analyzing the stability of the Poincaré map, where x^* is a fixed point, as presented in Equation 14. The main idea behind the HZD framework is that, due to the hybrid invariance of \mathbb{Z} , if there exists a stable hybrid periodic orbit, $\mathcal{O}_{\mathbb{Z}}$, for the reduced-order zero dynamics evolving on \mathbb{Z} (i.e., the restriction of $f_{\rm cl}$ to \mathbb{Z}), then $\mathcal{O}_{\mathbb{Z}}$ is a stable hybrid periodic orbit for the full-order dynamics in Equation 19 (16). Figure 9 presents a visualization of the components of HZD walking design.

In the case of robots that have feet, as is the case for many humanoid robots, one can extend the concept of HZD to modulate the forward velocity of the robot (103). In particular, one can generalize HZD through a velocity-modulating output: $y_1(q,\dot{q}) = y_1^a(q,\dot{q}) - v^d$, where v^d is the desired forward velocity. One can augment the original virtual constraints y(q) with this new (relative 1 degree) output. The partial HZD surface \mathbb{PZ} is again given as in Equation 19, where the term partial is used since this surface does not require the output y_1 to be zero. Partial HZD is the condition $\Delta_e(\mathbb{PZ} \cap S) \subset \mathbb{PZ}$. In the case of full actuation, the existence of a hybrid periodic orbit, \mathcal{O}_{PZ} in **PZ**, is guaranteed, implying the existence of a hybrid periodic orbit for the full-order dynamics. Thus, partial HZD implies the existence of a stable gait for fully actuated robots.

3.2.3. Application of hybrid zero dynamics. In the context of robotic implementations, HZD has proven successful in realizing a wide variety of dynamic behaviors. Many of the early uses of the method were on point-footed robots that were restricted to the sagittal plane. The first robot used to study HZD was the Rabbit biped (104), followed later by MABEL (105) and AMBER 1 (106). The ability of (partial) HZD to handle multidomain behaviors led to its use on more complex planar bipedal robots, such as ATRIAS (107, 108), AMBER 2 (109), and AMBER 3M (110). New challenges appeared while extending the method of HZD from planarized robots to 3D robots, which exhibit additional degrees of underactuation. Control of fully actuated humanoids was demonstrated on a small-scale example with a NAO robot (111) via partial HZD, while point-footed 3D walking with HZD was first shown at the University of Michigan with the MARLO biped (112). At the DARPA Robotics Challenge, the humanoid DURUS (shown in **Figure 10a**) was featured in an efficiency walk-off (20), where it demonstrated the first sustained

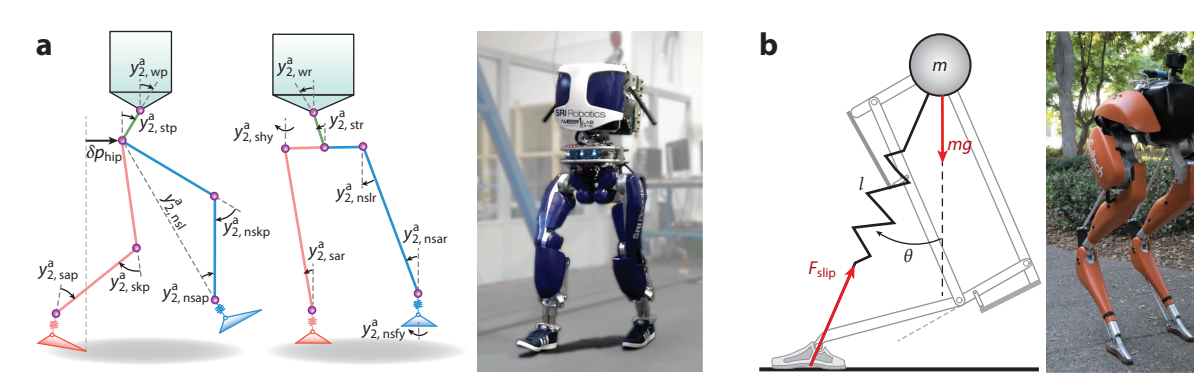


Figure 10

(a) Human-like outputs (103) applied to DURUS and (b) how the physical morphology of Cassie follows principles from SLIP models. Each robot then has passive dynamics, which can be embedded within the HZD framework via output selection. Abbreviations: HZD, hybrid zero dynamics; SLIP, spring-loaded inverted pendulum. Photo in panel a adapted from Reference 21 with permission from Springer; photo in panel b adapted from Reference 100 with permission from IEEE.

humanoid HZD walking—more than five hours continuously. DURUS went on to exhibit the most efficient walking on a humanoid to date, while performing human-like multicontact behaviors and managing significant underactuation (21). The method has been extended to powered prosthetic walking (113–115) and to exoskeletons that can walk for patients with paraplegia (116, 117). The use of springs in locomotion has also proven useful in the development of dynamic walking behaviors, though it presents additional challenges both mathematically and in practice. The notion of compliant HZD was introduced in the late 2000s (118) and was later expanded upon to obtain compliant robotic running (18).

One of the latest robots to successfully demonstrate stable HZD walking is the Cassie biped (shown in **Figure 2***a*), which exhibits underactuated feet and passive springs in the legs (see also the sidebar titled Experimental Highlight: Hybrid Zero Dynamics). Dynamic walking on Cassie has been successfully realized on hardware both by planning under the assumption of sufficient rigidity in the legs to ignore compliant elements (119) and by considering the passive compliance in the zero dynamics (100).

4. MOTION GENERATION FOR DYNAMIC BIPEDAL LOCOMOTION

Throughout the previous section, we outlined how the locomotion problem is fundamentally different from traditional approaches to modeling fixed-base robots. It is because of this inherent

EXPERIMENTAL HIGHLIGHT: HYBRID ZERO DYNAMICS

We highlight the application of HZD by considering its experimental realization on hardware. Leveraging partial HZD on DURUS and HZD on Cassie results in stable periodic orbits (both in simulation and experimentally), as illustrated in **Figure 7**. The evolution of the dynamic walking motion is tied to the morphology of the robot, with the humanoid DURUS exhibiting human-like heel—toe walking (21, 103) and the Cassie biped leveraging a domain structure and outputs that correspond to the SLIP-inspired mechanical design (100). In these specific examples, the virtual constraints chosen are shown in **Figure 10**. This demonstrates one of the benefits of HZD: the ability to choose virtual constraints to formally encoded reduced-order models for complex robots and correspondingly shape the zero dynamics surface to render it stable.

complexity that virtually all approaches to realizing dynamic walking must transcribe the locomotion problem into a motion planner that can handle the various constraints naturally imposed on the problem. While several of the more classical walking paradigms offer simple solutions to conservative walking, there has been a push over the last two decades toward leveraging optimization to obtain increasingly dynamic maneuvers.

4.1. Step Planning with Linear and Reduced-Order Models

For the simplest models of walking, such as traditional ZMP and LIPM versions of the capture point, the linear dynamics of the restricted system often yield straightforward approaches to planning the motion of the COM. The walking characterized by these linear models often implicitly satisfies quasi-static stability assumptions, ultimately allowing a control designer to decouple the high-level step planner and low-level balance controllers (120). In this vein, Kajita et al. (34) introduced the jerk of the COM as an input controlled by a discrete linear quadratic regulator controller with preview action (121) to plan ZMP trajectories for predefined footsteps. However, predefining the motions of the ZMP or footholds is not always necessary or desirable.

If planners for these simple models could instead be performed online, then the robot may be able to mitigate issues related to reactivity. Wieber (122) proposed using linear, trajectory-free model predictive control as a method for explicitly handling the constraints imposed by the ZMP approach of Section 2.2 while continuously reevaluating the walking path. Stephens & Atkeson (123) presented the use of model predictive control for push recovery and stepping on the SAR-COS humanoid, which could be extended to obtain walking behaviors. The example shown in Figure 3c visualizes the result of this approach applied to LIPM robotic walking. Studies have also shown how optimization and model predictive control can extend the notions of capture point to viable regions on which the biped can step (124) and how push recovery can be planned over a horizon of multiple steps (38). Despite the ability of these planners to adapt online, they cannot handle the discrete dynamics associated with foot strike, and they demand near-zero impact forces (125), which rules out the nontrivial impacts that are naturally associated with dynamic walking. It is also difficult to provide a priori guarantees on whether any given reduced-order plan is feasible to execute on the full-order dynamics. Such methods typically use inverse kinematics (126) or inverse dynamics (127), sometimes in an operational-space formulation (128), to compute the full-order control inputs at each instant. Solving such near-term inverse problems does not imply that future inverse problems in the trajectory will be feasible, which requires additional planning (129, 130).

4.2. Nonlinear Optimization for Gait Generation

As a result of the rapid developments within the trajectory optimization community, researchers began to move toward utilizing nonlinear dynamic gait optimizations rather than relying on the constraints imposed by linear modeling assumptions. The use of nonlinear optimization (i.e., numerical approaches) to generate stable walking behaviors on bipeds is not a new concept (131, 132), though computational limitations were a considerable hindrance to generating motions on 3D robots. During the mid-2000s, computation power finally increased sufficiently to begin handling 3D dynamic walking behaviors (133).

4.2.1. Open-loop optimization. Section 3.1 described the simplest application of nonlinear optimization to walking, wherein passive dynamic walking relies on the generation of fixed points associated with periodic orbits of a hybrid dynamical system. This naturally lends itself to

numerical approaches for the optimization of open-loop stable periodic motions (134), since passive dynamic walkers do not have any actuators to consider. The use of open-loop optimization to generate feasible motions for actuated robots is a natural extension of approaches used throughout the field of trajectory optimization, where the planning problem is seen as decoupled from the feedback control applied to the actual robot (135), and approximately optimal solutions are often sufficient. Furthermore, in recent years, the application of advanced trajectory optimization methods such as direct collocation has made the optimization of the full-body dynamics of Equation 1 more computationally tractable, sparking a growing interest in considering the full-body dynamics of the robot in the planning problem. For instance, in order to control the open-loop trajectory that results from the direct collocation optimization, a classical linear quadratic regulator-based feedback controller can be constructed to stabilize the resulting trajectory obtained for the constrained dynamical system (136). In this type of approach, the walking problem can be viewed as generating sequences of footholds for the nonlinear centroidal dynamics given in Equation 7 (40, 137) or with respect to the full Lagrangian system given in Equation 1 (138). Complementary Lagrangian systems (139) formed the basis of the approach used by Posa et al. (138), which allowed the optimizer to find walking behaviors without a priori enumeration of the type and order of contact events. Open-loop trajectory optimization has also been used to satisfy ZMP conditions in a nonlinear fashion (140), which considerably improved the dynamical nature of the conservative walking presented in Section 2.2.

4.2.2. Closed-loop optimization. While the preceding nonlinear optimization approaches do consider the full-body dynamics of the robot, it is not always desirable to apply feedback controllers to stabilize an approximately optimal open-loop plan. Rather, it is often beneficial to couple the gait generation and controller synthesis problems into a single framework: closed-loop optimization. This framework allows, among other things, the generation of provably stable walking behaviors that simultaneously satisfy the constraints on the system from admissible configurations to torque bounds. This idea forms the basis of designing walking gaits with the HZD method introduced in Section 3.2, where feedback control is used to generate provable stable periodic orbits. A visual summary of this section is given in **Figure 11** (see also the sidebar titled Experimental Highlight: Closed-Loop Optimization). Applying these closed-loop feedback strategies in the

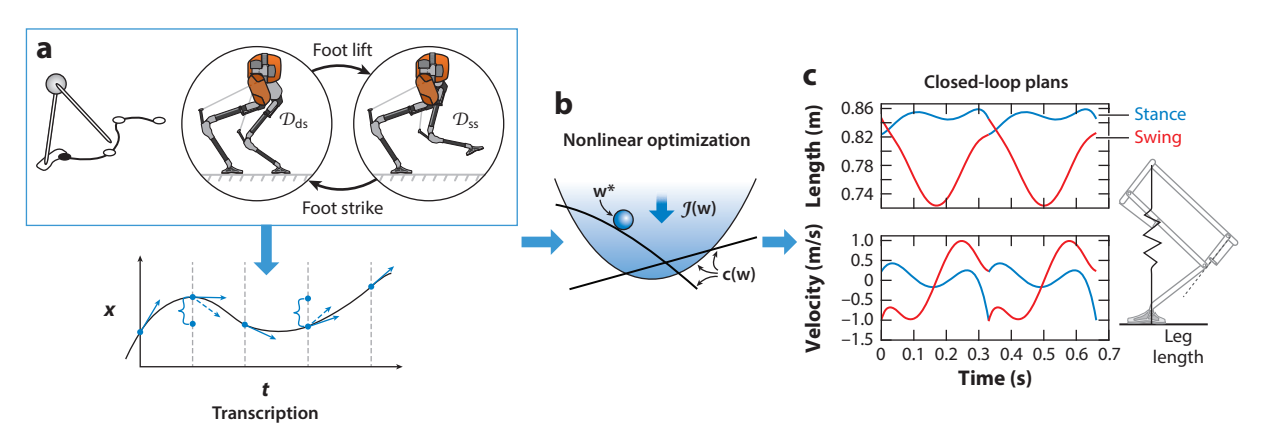


Figure 11

A conceptual illustration of how locomotion models must first be transcribed into appropriate representations for use with nonlinear programming approaches in order to yield dynamically stable closed-loop plans for bipedal robots. Some figure components adapted from References 21 and 100 with permission from Springer and IEEE, respectively.

EXPERIMENTAL HIGHLIGHT: CLOSED-LOOP OPTIMIZATION

The use of closed-loop optimization for HZD behaviors yields a set of outputs that coordinate the motion of the robot. This is shown as the output of the process in **Figure 11**, where the nonlinear optimization problem has provided outputs that yield orbital stability for compliant HZD (100). The outputs in **Figure 11** directly correspond to the SLIP-like morphology of the robot, emphasized in **Figure 10**. Reference trajectories can be shaped by the cost to yield desirable gait characteristics, such as efficiency on DURUS, or for minimizing torque and extraneous movement on Cassie to obtain behaviors that leverage the compliance for propulsion.

optimization problem means that ambiguous contact sequences are no longer possible (141) and must be prescribed according to the directed cycle that governs the underlying hybrid system (see **Figure 7**). Doing so allows one to enforce physical feasibility constraints (e.g., unilateral contact) in conjunction with the synthesis of controllers that guarantee stability.

In the context of HZD methods, with the formal constructions of the zero dynamics (Equation 19) and hybrid invariance (Equation 20) defined, the problem of finding stable dynamic walking can be transcribed to a nonlinear programming problem of finding a fixed point x^* and set of parameters $\alpha = \{\alpha_v\}_{v \in V}$ parameterizing the virtual constraints of Equation 15. The optimization problem is performed over one step cycle (e.g., foot strike to foot strike), with a constraint imposed such that when the discrete impact (Equation 13) is applied to the terminal state, it satisfies the hybrid invariance condition of Equation 20. It is also critical that the motions respect the limitations of the physical system, such as the friction cone (Equation 5), actuator limits, and joint limits. These constraints can be directly placed into a nonlinear programming problem that can be solved by a standard optimization solver:

$$\mathbf{w}(\alpha)^* = \underset{\mathbf{w}(\alpha)}{\operatorname{argmin}} \quad \mathcal{J}(\mathbf{w}(\alpha))$$
 21.
subject to closed-loop dynamics (Equation 18),
HZD condition (Equation 20),
physical feasibility (e.g., Equation 5),

where $\mathbf{w}(\alpha) \in \mathbb{R}^{N_w}$, with N_w being the total number of optimization variables, and here we made the dependence on the parameters, α , that dictate the closed-loop dynamics explicit. With the goal of achieving dynamic and efficient walking, a common objective is to minimize the mechanical cost of transport of the walking gait through the cost (20, 141). In classical HZD implementations, the candidate solutions were found via single-shooting formulations (15, 103), where the decision variables are the fixed-point states x^* and the output coefficients α . Because single-shooting optimizations are notoriously sensitive to poor initial conditions, multiple shooting has also been explored (142), with the eventual development of direct collocation formulations (143) that would become the most successful to date. The FROST optimization package (22) was developed based on these successes as an open-source package to transcribe HZD locomotion into a direct collocation problem. While the HZD optimization problem determines one stable walking orbit, one can expand the range of motions a robot can perform through systematic optimization in order to build libraries of walking parameters (144). Reinforcement learning has also been used to handle robust transitions for different speeds or unknown terrain height disturbances (145).

5. FEEDBACK CONTROL AND MOTION REGULATION

While the dynamic walking paradigms introduced throughout the previous sections generate stable walking motions in simulation, their actual implementation requires the deployment of real-time feedback controllers capable of achieving the desired motions. As described in Section 2.1, dynamic walking robots involve a high level of complexity in the form of nonlinearities and tightly coupled equations of motion that must be considered. When locomotion has been planned using a simplified model (Section 2.1), the spatial geometry of the robot must be translated into joint angles that can be controlled. Even with a full-order hybrid model (Section 3) and closed-loop optimization (Section 4), controllers must be synthesized in order to track these desired motions in practice. This section describes feedback controllers and motion regulators that allow the translation of dynamic walking in simulation to be realized on real-world hardware platforms.

5.1. Controllers for Tracking Designed Motions

The simplest control scheme for determining motor torques is proportional—derivative (PD) control (146). The strongest argument for using this approach is the sheer simplicity of its implementation and its intuitive physical meaning with respect to tuning. Consider the desired positions and velocities q^d and \dot{q}^d (and possibly functions of time), obtained either from inverse kinematics for reduced-order walking models or from the output of an optimization problem. A feedback controller can be applied at the joint level:

$$u = -K_{\rm p}(q^{\rm a} - q^{\rm d}) - K_{\rm d}(\dot{q}^{\rm a} - \dot{q}^{\rm d}),$$
 22.

generating desired torques (or currents) that are tracked at the motor controller level at a fast loop rate. In the case of underactuated robots and/or virtual constraints (see Section 3.2.1), one can consider outputs of the form

$$y(q) = y^{a}(q) - y^{d}(\tau(q), \alpha)$$
 or $y(q, t) = y^{a}(q) - y^{d}(\tau(t), \alpha),$

where the time-based variant is often considered in practice, especially in the case of 3D walking and running, due to imperfect sensing of $\tau(q)$, wherein it is replaced by the more robust signal $\tau(t)$ (19, 147). Let $q_{\rm m}$ represent the joints with actuators; then the PD controller can be applied in the Cartesian (or output) space:

$$u = -Y(q)^{-1}(K_{p}y + K_{d}\dot{y})$$
 or $u = -Y(q)^{T}(K_{p}y + K_{d}\dot{y}),$ 23.

where $Y(q) := \frac{\partial y^a}{\partial q_m}(q)$ is the Jacobian of the Cartesian task or output with respect to the actuated joints, and K_p and K_d are the PD gain matrices. This style of feedback control has been used to enforce the behaviors of every locomotion paradigm detailed in Sections 2 and 3 at some point in time.

For underactuated dynamic walkers whose motions have been planned with virtual constraints, simply tracking the outputs with a well-tuned PD controller is sometimes sufficient to achieve walking (21, 100, 105, 144, 148) and even running (19) on hardware. This is because the trajectories (or outputs) implicitly encode the dynamic behavior and stability constraints, even if achieving these behaviors requires different torques on the actual robot. In addition, because dynamic behaviors are often rendered stable through this behavioral encoding while satisfying appropriate physical constraints, almost all passive dynamic and HZD walkers have not included load cells in the feet, as feedback control of these quantities is not necessary for stability. **Figure 12** shows an example of PD controllers applied in experiment to two 3D bipedal robots; although the motions do not track the designed motions perfectly, they do form a closed orbit, which implies stable walking.

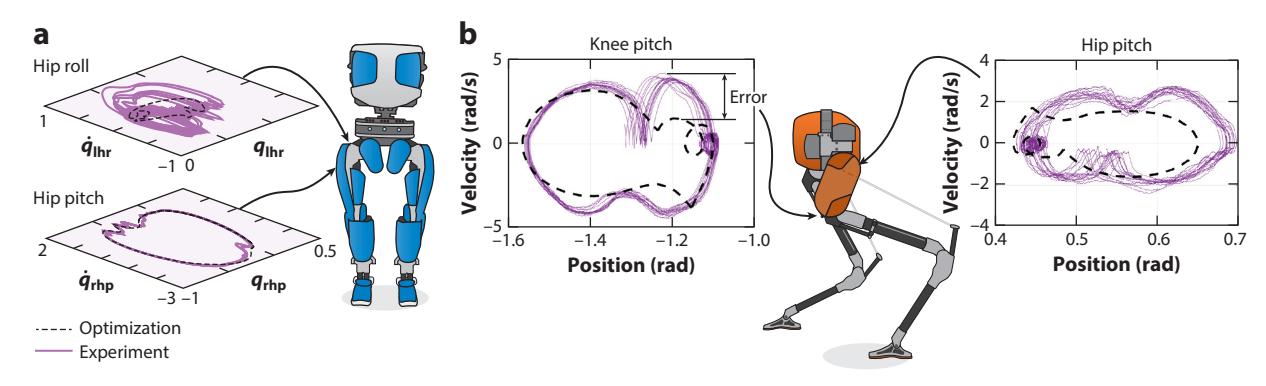


Figure 12

Examples of HZD periodic orbits for dynamic walking on hardware with the (a) DURUS and (b) Cassie robots. The nominal periodic walking motions resulting from the optimization (Equation 21) are shown as dashed lines and superimposed on traces of experimental data. Abbreviation: HZD, hybrid zero dynamics. Panel a adapted from Reference 21 with permission from Springer; panel b adapted from Reference 100 with permission from IEEE.

In the context of reduced-order models, plans for the ZMP and the capture point have typically considered a point-mass representation of the robot, under which whole-body momentum and force regulation become important concerns when developing feedback controllers for implementation. This has led to a variety of approaches that concurrently regulate the COM movement via some PD feedback element in combination with control of the whole-body momentum (149–152) and tracking of desired force interactions (153, 154).

When the dynamics of the system are well known, it is often beneficial to leverage them in the feedback control design. One of the classical methods used to explore this in the context of bipedal robots is computed-torque control, which considers an inner nonlinear compensation loop and the design of an auxiliary control feedback (43, 155):

$$u = D(q) \left(\ddot{q}^* - K_p(q - q^d) - K_d(\dot{q} - \dot{q}^d) \right) + H(q, \dot{q}),$$
 24.

where \ddot{q}^* is the nominal system acceleration. Note that this is mathematically equivalent to feedback linearization, as given in Equation 17 (see 156). Although both the standard PD controller and computed-torque approach can overcome minor disturbances, they are often not sufficient to formally ensure the stability or yield the performance that dynamic walking requires. This motivates the use of a controller that can provide good tracking performance while leveraging the robotic model (see also the sidebar titled Experimental Highlight: Trajectory Tracking along with **Figure 13**). The remainder of this section will explore several of the approaches that have been successful in the feedback control of bipedal robots, and how these can be extended to provide formal stability guarantees.

EXPERIMENTAL HIGHLIGHT: TRAJECTORY TRACKING

The trajectories found in Section 4.2 for HZD are well suited to feedback controllers for output-tracking problems. To demonstrate the simplest and yet effective implementations of PD controllers that have been successful in realizing dynamic walking, we show experimental results on hardware for DURUS and Cassie in **Figure 13**. This figure shows that for controllers in the joint space (Equation 22) and output space (Equation 23), dynamic walking can be achieved by simply tracking the designed motion.

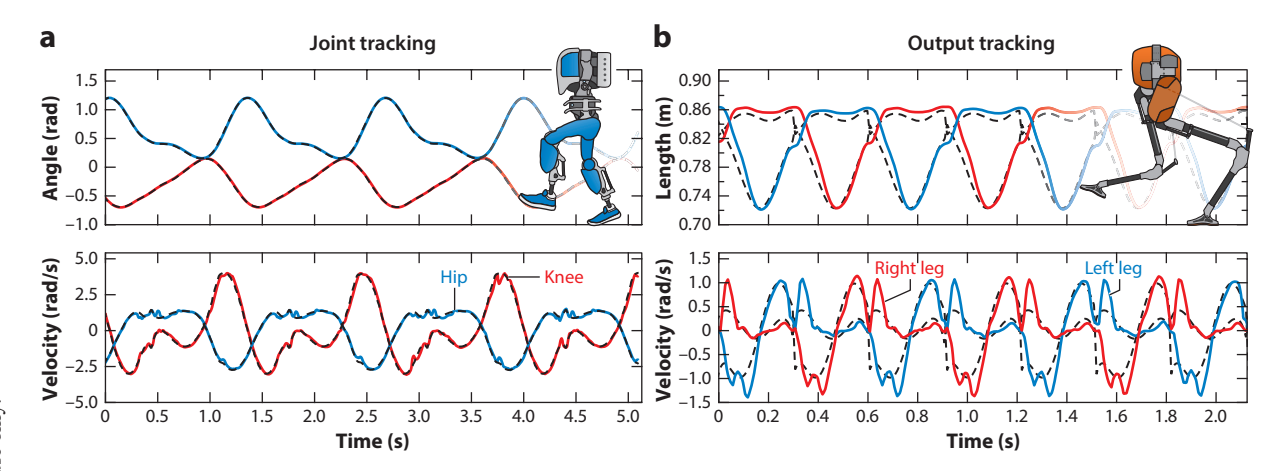


Figure 13

Examples of experimental results for the use of PD control for tracking dynamic walking on hardware. (a) Joint tracking (Equation 22) for DURUS during multicontact walking (21). (b) Leg length output tracking (Equation 23) on Cassie while walking with a compliant HZD gait (100). Abbreviations: HZD, hybrid zero dynamics; PD, proportional—derivative.

5.1.1. Inverse dynamics. While PD control is sufficient for many applications, it fails to explicitly consider the model of the robot and the constraints under which it operates. Inverse dynamics is a widely used approach to model-based controller design for achieving a variety of motions and force interactions, typically in the form of task-space objectives. Given a target behavior, the dynamics of the robotic system are inverted to obtain the desired torques. In most formulations, the system dynamics are mapped onto a support-consistent manifold using methods such as the dynamically consistent support null space (157), linear projection (158), and orthogonal projection (159). When prescribing behaviors in terms of purely task-space objectives, this method is commonly referred to as task- or operational-space control (128). Recent work has shown that variations of these approaches allow high-level tasks to be encoded with intuitive constraints and costs in optimization-based controllers (e.g., 40, 152, 160–162).

A benefit of inverse dynamics approaches to feedback control on robotic systems is that low-gain feedback control can be used, while feedforward terms that respect the constrained rigid-body dynamics of the physical system are used to produce the majority of the control action. If the walking is not significantly disturbed from the planned motion found in Section 4.2, then a linear null-space projection operator $P_F(q)$ can be used to eliminate the contact forces λ from the floating-base dynamics in Equation 1 (158), using QR decomposition (159) to obtain an orthogonal projection into the null space of $J_h(q)$.

The inverse dynamics problem can also be posed using a quadratic program to exploit the fact that the instantaneous dynamics and contact constraints can be expressed linearly with respect to a certain choice of decision variables. Specifically, let us consider the set of optimization variables $\mathcal{X} = [\ddot{q}^T, u^T, \lambda^T]^T \in \mathbb{X}_{\text{ext}} := \mathbb{R}^n \times U \times \mathbb{R}^{m_h}$, which are linear with respect to Equations 1 and 4,

$$\begin{bmatrix} D(q) & -B & -J_{h}(q)^{\mathrm{T}} \\ J_{h}(q) & 0 & 0 \end{bmatrix} \mathcal{X} + \begin{bmatrix} H(q, \dot{q}) \\ \dot{J}_{h}(q) \dot{q} \end{bmatrix} = 0,$$
 25.

and a positional objective in the task space of the robot written as $J_y(q)\ddot{q} + \dot{J}_y(q,\dot{q})\dot{q} - \ddot{y}_2^* = 0$, where $J_y(q) = \partial y^a/\partial q$, and $\ddot{y}^* = K_P y + K_D \dot{y}$ is a PD control law that can be tuned to achieve convergence. An additional benefit to using an optimization-based approach is the ability to include feasibility constraints such as the friction cone (Equation 5). However, this constraint is nonlinear and cannot

be implemented as a linear constraint. An alternative solution is to use a pyramidal friction cone approximation (26),

$$\mathcal{P} = \left\{ (\lambda_x, \lambda_y, \lambda_z) \in \mathbb{R}^3 \middle| \lambda_z \ge 0; |\lambda_x|, |\lambda_y| \le \frac{\mu}{\sqrt{2}} \lambda_z \right\},$$
 26.

which is a more conservative model than the friction cone but is advantageous in that it is a linear inequality constraint. In its most basic case, we can combine these elements to pose this quadratic program tracking problem as

$$\mathcal{X}^*(x) = \underset{\mathcal{X} \in \mathbb{X}_{\mathrm{ext}}}{\operatorname{argmin}} \quad ||J_y(q)\ddot{q} + \dot{J}_y(q,\dot{q})\dot{q} - \ddot{y}^*||^2 + \sigma W(\mathcal{X})$$
 subject to Equation 25 (system dynamics),
$$u_{\min} \leq u \leq u_{\max} \text{ (torque limits)},$$
 Equation 26 (friction pyramid),

where $W(\mathcal{X})$ is included as a regularization term with a small weight σ such that the problem is well posed. Although this kind of control satisfies the contact constraints of the system and yields an approximately optimal solution to tracking task-based objectives, it does not provide formal guarantees with respect to stability. In increasingly dynamic walking motions, this becomes an important consideration, wherein impacts and foot strike can destabilize the system, requiring more advanced nonlinear controllers.

5.1.2. Control Lyapunov functions for zeroing outputs. The methods presented thus far demonstrate how feedback control can drive the dynamics of the robotic system to behave according to the planned motions found in Section 4. However, these designs often intrinsically ignore the natural dynamics of the system, which are a critical component in the realization of efficient and dynamic walking. Thus, for practical systems, additional considerations for selecting the control input are often required. Rapidly exponentially stabilizing control Lyapunov functions (RES-CLFs) were introduced as methods for (rapidly) achieving exponential stability for walking robots (17, 163). A function, *V*, is a RES-CLF if it satisfies

$$\underline{\gamma} \|x\|^2 \le V_{\epsilon}(x) \le \frac{\overline{\gamma}}{\epsilon^2} \|x\|^2,$$
 27.

$$\inf_{u \in U} \left[\dot{V}_{\epsilon}(x, u) \right] = \inf_{u \in U} \left[\underbrace{\frac{\partial V_{\epsilon}}{\partial x}(x) f(x)}_{L_{f} V_{\epsilon}(x)} + \underbrace{\frac{\partial V_{\epsilon}}{\partial x}(x) g(x)}_{L_{g} V_{\epsilon}(x)} u \right] \le -\frac{\gamma}{\epsilon} V_{\epsilon}(x),$$
28.

for $\underline{\gamma}, \overline{\gamma}, \gamma > 0$, where $0 < \epsilon < 1$ is a control gain that allows one to control the exponential convergence of the CLF and is the basis for the term rapid in RES-CLF. Importantly, if the robotic system is feedback linearizable per Section 3.2, it automatically yields a Lyapunov function. In particular, defining $\eta(x) := (y(x)^T, \dot{y}(x)^T)^T$, we obtain the RES-CLF $V_{\epsilon}(x) = \eta(x)^T P_{\epsilon} \eta(x)$, where $P_{\epsilon} = \mathbf{I}_{\epsilon} P \mathbf{I}_{\epsilon}$, with $\mathbf{I}_{\epsilon} := \operatorname{diag}\left(\frac{1}{\epsilon}\mathbf{I},\mathbf{I}\right)$ and P the solution to the continuous-time algebraic Riccati equations for the linear system $\ddot{y} = \mu$ obtained by feedback linearization in Equation 17.

The advantage of using CLFs for controller synthesis is that they yield an entire class of controllers that provably stabilize periodic orbits for hybrid system models of walking robots and can be realized in a pointwise optimal fashion via optimization-based controllers. In particular,

consider the set of control inputs

$$K_{\epsilon}(x) = \{ u \in U : L_f V_{\epsilon}(x) + L_g V_{\epsilon}(x) | u \le -\frac{\gamma}{\epsilon} V_{\epsilon}(x) \},$$
 29.

which is a set of stabilizing controllers. To see this, note that for $u^*(x) \in K_{\epsilon}(x)$,

$$\dot{V}_{\epsilon}(x, u^{*}(x)) \leq -\frac{\gamma}{\epsilon} V_{\epsilon}(x) \qquad \Rightarrow \qquad V(x(t)) \leq e^{-\frac{\lambda}{\epsilon}t} V(x(0))
\Rightarrow \qquad \|\eta(x(t))\| \leq \frac{1}{\epsilon} \sqrt{\frac{\lambda_{\max}(P)}{\lambda_{\min}(P)}} e^{-\frac{\gamma}{2\epsilon}t} \|\eta(0)\|.$$

Thus, this gives the set of control values that exponentially stabilize the outputs, and we can control the convergence rate via ϵ . The selection of an appropriate choice for the best control value possible leads to the notion of optimization-based control with CLFs.

The advantage of Equation 29 is that it gives a set of controllers that result in stable walking on bipedal robots. That is, for any $u \in K(x)$, the hybrid system model of the walking robot, per the HZD framework introduced in Section 3.2, has a stable periodic gait given a stable periodic orbit in the zero dynamics (17). This suggests an optimization-based framework for nonlinear controller synthesis, with specific application to dynamic locomotion. Specifically, the optimization formulation of CLFs allows for additional constraints and objectives to be applied as a quadratic program with the form (as first introduced in Reference 156)

$$\begin{split} u^* &= \underset{u \in U \subset \mathbb{R}^m}{\operatorname{argmin}} \quad u^{\mathrm{T}} H(x) u + \rho \delta^2 \\ &\text{subject to} \quad L_f V_\epsilon(x) + L_g V_\epsilon(x) u \leq -\frac{\gamma}{\epsilon} V_\epsilon(x) + \delta \text{ (CLF convergence)}, \\ &\quad u_{\min} \leq u \leq u_{\max} \text{ (torque limits)}, \\ &\quad \text{Equation 26 (friction pyramid)}, \end{split}$$

where H(x) is a user-specified positive-definite cost, δ is a relaxation to the convergence constraint that can be added if infeasibility of the solution is a concern, and $\rho > 0$ is a large value that penalizes violations of the CLF constraint. If the relaxation term is included, then the formal guarantees on convergence are no longer satisfied in lieu of achieving pointwise optimal control actions that satisfy the physical constraints of the robot. Ground reaction forces on the robot also appear in an affine fashion in the dynamics; thus, one can also use the CLF-based quadratic program framework in the context of force control (156).

The CLF-based controllers presented throughout this section have recently been explored for application on hardware because, much like the optimization controllers of Section 5.1.1, they can be solved in real time. Experimental results have been shown on MABEL (17, 164) and DURUS-2D (165), with recent results indicating how robust formulations can be used (166) and how alternative representations can make the problem more tractable for implementation on 3D robots (167). Additionally, a CLF-based controller was implemented at over 5 kHz as an embedded-level controller on series-elastic actuators (168), indicating possible future uses for explicitly controlling compliant dynamic walking. CLFs have also been used to automatically generate stable walking gaits through SLIP approximations (169), to enforce planned motions for reduced-order models (170), and to realize 3D bipedal jumping experimentally on Cassie (171) (see also the sidebar titled Experimental Highlight: Real-Time Quadratic Program Control Using Control Lyapunov Functions along with Figure 14).

EXPERIMENTAL HIGHLIGHT: REAL-TIME QUADRATIC PROGRAM CONTROL USING CONTROL LYAPUNOV FUNCTIONS

We highlight the application of CLF-based quadratic programs on hardware in real time in the context of dynamic crouching maneuvers on Cassie, shown in **Figure 14** (100). Because the CLF quadratic program can be run at a sufficient control frequency (in this case, at 1 kHz), these experiments show how convergence properties combined with inclusion of the model can lead to desirable tracking performance on complex bipedal robots. These methods are directly extensible to tracking walking trajectories, where the constrained pointwise optimization can select torques that satisfy the contact constraints governed by the discrete structure of the hybrid system model (see **Figure 7**).

5.2. Stabilizing Walking with Trajectory Modification

The previous sections have detailed how dynamic walking behaviors are formulated, synthesized, and tracked; however, these components alone are often not sufficient to realize sustained and robust robotic walking on hardware. The final step in achieving robustness involves the artful implementation of modifying the desired behavior to account for unknown and unmodified disturbances—both specific to the hardware (e.g., unmodified compliance) and in the external environment (e.g., rough terrain). Approaches such as model predictive control planners and analytical expressions for the capture point, presented in Section 4.1, can be evaluated in real time to adapt the motion of the robot to avoid falling or recover from large pushes (123). In these cases, the planning and the real-time compensation are inherently tied (172), though they are still replanning over an approximate model of the robot and can lead to constrained motions that are prohibitive to truly dynamic walking. On the other hand, while the nominal trajectories of offline plans that consider the full-body continuous and hybrid dynamics are generated with high-fidelity models (such as the motions found via Section 4.2), it is evident in experimental trials that some additional feedback is crucial to stabilizing the robot for sustained periods of walking. These nominal trajectories are often superimposed with some form of regulator in order to overcome

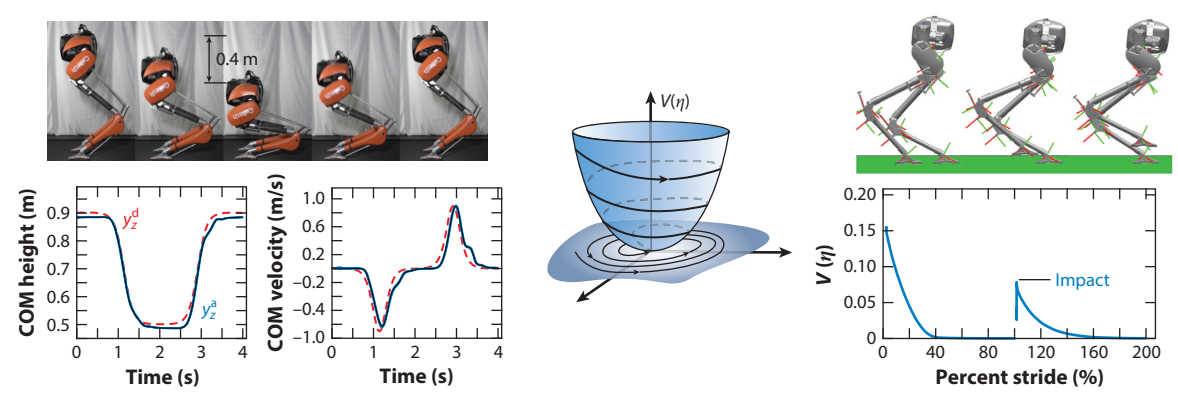


Figure 14

A CLF driving a Lyapunov function to zero, with data from an experimental implementation shown on the left and data from a walking simulation shown on the right. Because CLFs consider the model to enforce convergence, outputs are closely tracked with minimal error (*left*). The rapid exponential zeroing the outputs (Equation 30) is critical to achieve sufficient convergence before impact (*right*). Abbreviation: CLF, control Lyapunov function. Walking tiles adapted from Reference 167 with permission from IEEE.

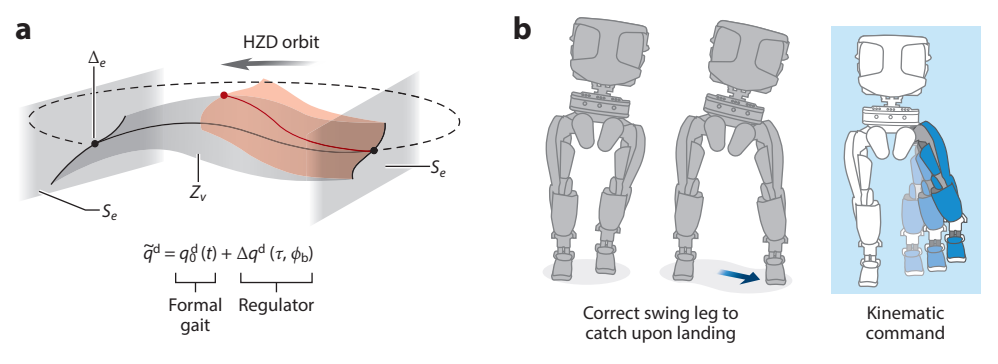


Figure 15

How a regulator action is used to drive a perturbed zero dynamics surface back to the nominal motion. This action (as shown in panel a) can take the form of direct joint changes or Cartesian foot placement (as shown in panel b), making a kinematic adjustment in response to torso lean or velocity. Panel b adapted from Reference 21 with permission from Springer.

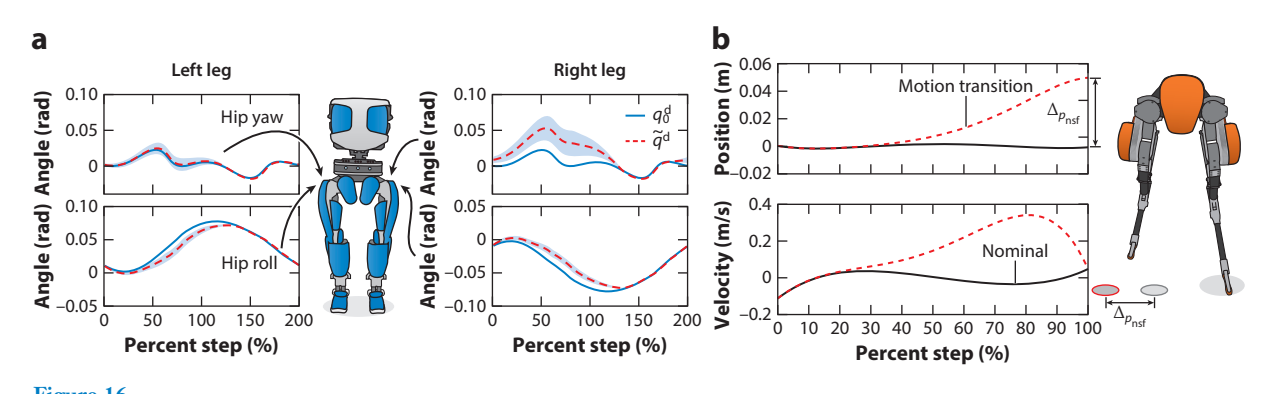
uncertainties due to model mismatch and tracking errors, typically in the form of adding trajectory-level feedback (see Figure 15). The development of these regulators is a largely heuristic task but has often proven critical to stability on hardware. A variety of different regulators have proven useful, though the implementation depends largely on the robotic system and desired behavior.

When performing dynamic maneuvers, it is inevitable that the actual linkages of humanoid robots, which have large masses and inertias, can subject rotational joints to backlash and unsensed compliance. For these problems, using an experimentally measured stiffness coefficient to augment commanded positions based on anticipated torque at the joint can be an effective compensation strategy (21, 39). The combination of uncertainty in the kinematics and dynamics of the robot can also lead to predictable issues with gait timing on periodic walking behaviors. For dynamic walking that has been planned with a monotonic phase variable $\tau(q)$ that is dependent on the state of the robot, there can be a large amount of uncertainty regarding the estimation of the floating-base coordinates and therefore the phase (19, 147). In these cases, it can be beneficial to employ a combination of time- and state-based progression of the variable (144).

Another type of regulation comes in the form of small modifications to the shape of the robot (i.e., superimposed perturbations to virtual constraints) from stride to stride. How this can be conceptually interpreted within the HZD framework is shown in Figure 15, where control designers seek to shape a perturbed zero dynamics surface such that the hybrid system returns to an orbit that satisfies hybrid invariance. In early developments for control of HZD walking, the restricted Poincarè map was viewed as a discrete-time control system (173). Through consideration of the linearized map at the fixed point x^* (see Equation 14), a discrete linear quadratic regulator algorithm can be used to acquire a feedback gain to modify the configuration of the next foot strike (108). This can be straightforward to design for 2D robots, but extensions to 3D become more difficult. Perhaps the most common approach is to instead utilize foot-placement routines inspired by Raibert et al. (11). This simple deadbeat step-to-step controller most often takes the form of a discrete PD controller to augment the foot-strike locations in the sagittal and frontal planes during locomotion:

$$\Delta p_{\text{nsf}} = \tilde{K}_{\text{p}}(\bar{v}_k - v_{\text{ref}}) + \tilde{K}_{\text{d}}(\bar{v}_k - \bar{v}_{k-1}), \qquad 31.$$

where the average velocity of the current step \bar{v}_k and previous step \bar{v}_{k-1} are computed directly from an estimate of the floating-base velocity, and the reference velocity $v_{\rm ref}$ is taken from the



(a) Experimental data from walking on the DURUS humanoid (20), where the shaded region is 1 standard deviation of more than 200 steps. Trajectories are modified by a regulator proportional to torso lean. (b) An example of a motion transition (174) applied to an output for the swing foot position. Panel a adapted from Reference 21 with permission from Springer.

nominal trajectory. In addition, because outputs for HZD walking are typically parameterized by a Bézier polynomial, the update value $\Delta p_{\rm nsf}$ can directly augment the last two parameters of the corresponding output polynomials (174). This kind of smooth transition is demonstrated in **Figure 16***b*, where the position has been smoothly modified but the velocity at impact will remain the same.

This simple foot-placement regulator has been successfully implemented on several dynamic walking robots (100, 144, 175). Rather than considering hand-tuned regulation, Griffin & Grizzle (176) introduced the notion of nonholonomic virtual constraints, aiming to formalize a representation of virtual constraints that are insensitive to a predetermined and finite set of terrain variations and velocity perturbations. Implementation of this approach required intensive optimizations, as the walking was made to be stable amid a variety of perturbations in each step of the optimization. This type of output-level feedback has also been successful in a more directly hand-tuned fashion, as in work by Reher et al. (20, 21), where the position-level feedback of the outputs was governed by a proportional gain with respect to the pitch and roll of the robot's torso. The superimposed motion will then be zero if the walking is directly on the orbit but will smoothly apply a superimposed positional command if necessary. One interpretation of this regulator feedback is simply that y_a has been made a function of the floating-base coordinates of the robot, with an example shown on the DURUS humanoid in **Figure 16a** (see also the sidebar titled Experimental Highlight: Dynamic Walking along with **Figure 17**).

6. CONCLUDING REMARKS

This review has outlined the general methodology for achieving dynamic walking on bipedal robots. As outlined in the Summary Points below, we began by considering reduced-order models that capture the essentials of locomotion, although they are not sufficient for handling the full complexity of walking robots. This led to full-order models that include impacts, as represented by hybrid systems, wherein we considered HZD. We then discussed the role of optimization in using these models to generate walking gaits and corresponding dynamically feasible trajectories. Finally, connecting models with walking gaits, we discussed real-time controllers that enable hardware realization, ranging from simple control methods to advanced quadratic program—based controllers, together with the modification of these nominal desired values due to uncertainty in the system and environment. This end-to-end process was illustrated throughout on the bipedal

EXPERIMENTAL HIGHLIGHT: DYNAMIC WALKING

The experimental highlights considered throughout this article culminate with efficient and agile locomotion on DURUS and Cassie, as shown in **Figure 17**. The multicontact walking on DURUS demonstrated efficiency, as evidenced by an exceptionally low cost of transport (21), which was achieved by leveraging hybrid models, closed-loop optimization, and real-time feedback controllers and regulators. The compliant walking on Cassie (100) demonstrated agility through a wide range of walking speeds up to 1 m/s, along with the ability to walk on unplanned rough terrain outdoors.

robots DURUS and Cassie, highlighting the translation to hardware and corresponding experimental results.

The process of realizing efficient and agile dynamic walking is ripe with opportunities, some of which are highlighted in the Future Issues box below. In essence, the challenges can be divided into two categories: theoretical and practical. The overarching goal, theoretically, is to formally and holistically extend the methodologies presented. The hope is to, as a result, develop a framework that can realize aperiodic dynamic motions (177, 178) that are stable and safe (179), planned in real time (180), and robust to uncertainties in the robot and environment. From a practical perspective, hardware is constantly improving and becoming more accessible, enabling approaches for agile and efficient walking to be better tested in real-world scenarios. The goal is to finally realize the promise of dynamic walking: imbuing legged robots with the locomotion capabilities that will enable them to do everything from traversing everyday environments to exploring the cosmos.

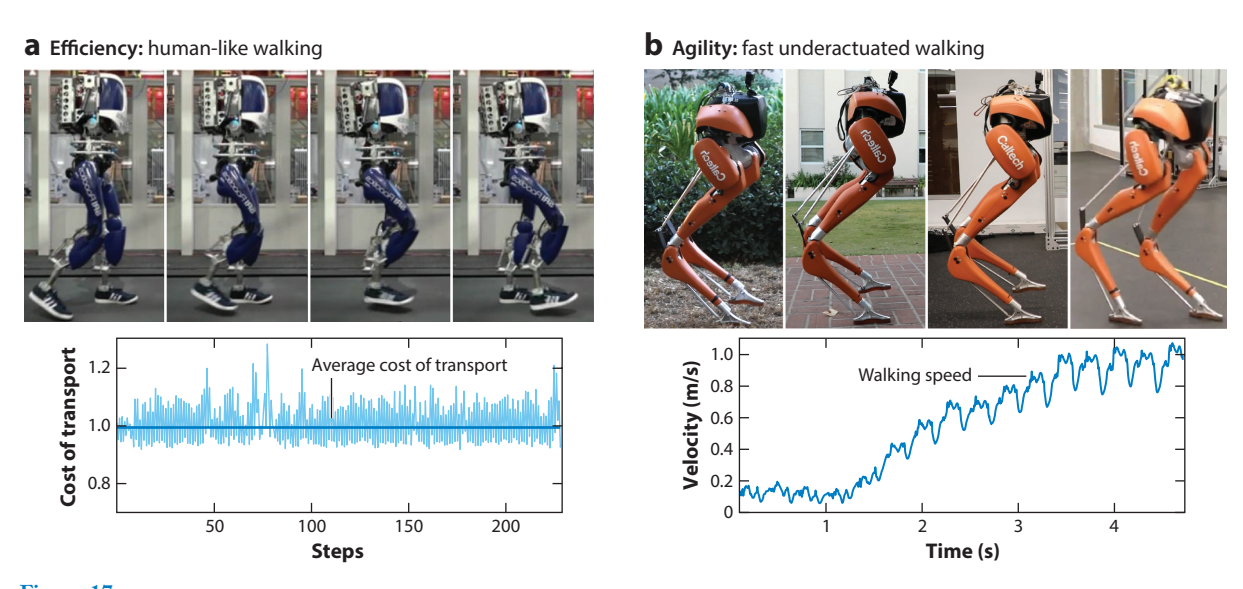


Figure 17

Experimental examples of dynamic walking on (a) DURUS and (b) Cassie. Gait tiles are provided, showing the robots in various phases of their natural strides, along with a plot of data detailing the walking efficiency for DURUS and a plot of the sagittal walking velocity for Cassie. Panel a adapted from Reference 21 with permission from Springer; gait tiles in panel b adapted from Reference 100 with permission from IEEE.

SUMMARY POINTS

- Reduced-order models: At the core of dynamic walking is the idea of reduced-order models. These are either hierarchical (representing desired behavior on simple models, such as inverted pendula and compass gait bipeds) or formally determined (lowdimensional systems rendered invariant by controllers, such as hybrid zero dynamics).
- Full-order nonlinear dynamics: Bipedal robots are inherently nonlinear with hybrid dynamical behaviors. These full-order dynamics must be accounted for through assumptions that yield reduced-order models, through nonlinear controllers, or through optimization algorithms.
- 3. Optimization for gait generation: Reduced-order models must be instantiated on the full-order dynamics via optimization algorithms. This can leverage reduced-order models, exploit the full-order dynamics, or any combination thereof. Algorithms that allow these optimization problems to be solved efficiently are essential in instantiating walking gaits on hardware platforms.
- 4. Control laws for hardware realization: Control laws allow for the generated gaits to ultimately be realized on hardware. These can range from simple control laws to complex nonlinear real-time optimization-based controllers and can be modulated via inspiration from reduced-order models. These control algorithms are the final step in realizing dynamic walking on bipedal robots.

FUTURE ISSUES

- Generalized notions of stability and safety: The walking considered herein (and the notions of stability) was largely periodic in nature. To better represent a wide variety of behaviors, the idea of stability should be extended to include aperiodic walking motions. More generally, safety as represented by set invariance could provide a powerful tool for more generally understanding locomotion.
- 2. Real-time optimal gait planning: Nonlinear constraint optimization plays an essential role in generating dynamic walking behaviors that leverage the full-body dynamics. These methods have become highly efficient, even allowing for online calculation in simple scenarios. Further improving computational efficiency will enable real-time implementation, yielding new paradigms for gait generation.
- 3. Bridging the gap between theory and practice: As indicated by the methods discussed in Section 5, there is often an artful-implementation step that translates model-based controllers to a form that can actually be implemented on hardware. Ideally, methods can be developed that allow the exact transcription of model-based methods to hardware in a robust fashion and without heuristics.
- 4. Robustness, adaptation, and learning: Dynamic walking behaviors often work in isolated instances and predefined environments. Translating these ideas to the real world will require robustness to uncertainty, both in the internal dynamics and in the external environment. Adaptive and learning-based controllers can help mitigate model uncertainty and unplanned interactions with the world, from uncertain contact conditions to walking on surfaces with complex interactions (e.g., sand).

5. Real-world deployment of bipedal robots: The ultimate challenge is the ability to deploy bipedal robots in real-world scenarios, ranging from everyday activities, to aiding humans, to venturing into dangerous environments. Examples include bipedal robotics in healthcare settings (e.g., exoskeletons for restoring mobility) and humanoid robots capable of exploring Mars.

DISCLOSURE STATEMENT

The authors are not aware of any affiliations, memberships, funding, or financial holdings that might be perceived as affecting the objectivity of this review.

ACKNOWLEDGMENTS

The authors would like to thank the members of the Advanced Mechanical Bipedal Experimental Robotics (AMBER) Lab who have contributed to the understanding of robotic walking summarized in this article. Of special note are Shishir Kolathaya, Wenlong Ma, Ayonga Heried, Eric Ambrose, and Matthew Powell for their work on AMBER 1, 2, and 3M and DURUS, from developing the theory and computational methods to carrying out the experimental realization. Outside of AMBER Lab, the authors would like to thank their many collaborators, particularly Jessy Grizzle for his joint work on HZD and CLFs. This work was supported over the years by the National Science Foundation, including awards CPS-1239055, CNS-0953823, NRI-1526519, CNS-1136104, and CPS-1544857. Other support includes projects from NASA, DARPA, SRI, and Disney.

LITERATURE CITED

- 1. Lim HO, Takanishi A. 2007. Biped walking robots created at Waseda University: WL and WABIAN family. Philos. Trans. R. Soc. A 365:49-64
- 2. Vukobratović M, Hristic D, Stojiljkovic Z. 1974. Development of active anthropomorphic exoskeletons. Med. Biol. Eng. 12:66-80
- 3. Vukobratović M, Stepanenko J. 1972. On the stability of anthropomorphic systems. Math. Biosci. 15:1-37
- Vukobratović M, Borovac B. 2004. Zero-moment point—thirty five years of its life. Int. J. Humanoid Robot. 1:157-73
- 5. Collins S, Ruina A, Tedrake R, Wisse M. 2005. Efficient bipedal robots based on passive-dynamic walkers. Science 307:1082-85
- 6. Hirose M, Ogawa K. 2007. Honda humanoid robots development. Philos. Trans. R. Soc. A 365:11-19
- 7. Kaneko K, Kanehiro F, Kajita S, Yokoyama K, Akachi K, et al. 2002. Design of prototype humanoid robotics platform for HRP. In IEEE/RSJ International Conference on Intelligent Robots and Systems, pp. 2431–36. Piscataway, NJ: IEEE
- 8. Akachi K, Kaneko K, Kanehira N, Ota S, Miyamori G, et al. 2005. Development of humanoid robot HRP-3P. In 5th IEEE-RAS International Conference on Humanoid Robots, pp. 50-55. Piscataway, NJ: IEEE
- 9. Ito Y, Nozawa S, Urata J, Nakaoka T, Kobayashi K, et al. 2014. Development and verification of lifesize humanoid with high-output actuation system. In 2014 IEEE International Conference on Robotics and Automation, pp. 3433-38. Piscataway, NJ: IEEE
- 10. Park IW, Kim JY, Lee J, Oh JH. 2005. Mechanical design of humanoid robot platform KHR-3 (KAIST Humanoid Robot 3: HUBO). In 5th IEEE-RAS International Conference on Humanoid Robots, pp. 321-26. Piscataway, NJ: IEEE

- Raibert MH, Brown HB Jr., Chepponis M. 1984. Experiments in balance with a 3D one-legged hopping machine. Int. 7. Robot. Res. 3:75–92
- 12. Raibert MH. 1986. Legged Robots That Balance. Cambridge, MA: MIT Press
- 13. Hürmüzlü Y, Moskowitz GD. 1986. The role of impact in the stability of bipedal locomotion. *Dyn. Stab.* Syst. 1:217–34
- 14. McGeer T. 1990. Passive dynamic walking. Int. J. Robot. Res. 9:62-82
- Westervelt ER, Grizzle JW, Koditschek DE. 2003. Hybrid zero dynamics of planar biped walkers. IEEE Trans. Autom. Control 48:42–56
- Westervelt ER, Grizzle JW, Chevallereau C, Choi JH, Morris B. 2018. Feedback Control of Dynamic Bipedal Robot Locomotion. Boca Raton, FL: CRC
- Ames AD, Galloway K, Sreenath K, Grizzle JW. 2014. Rapidly exponentially stabilizing control Lyapunov functions and hybrid zero dynamics. IEEE Trans. Autom. Control 59:876–91
- Sreenath K, Park HW, Poulakakis I, Grizzle JW. 2013. Embedding active force control within the compliant hybrid zero dynamics to achieve stable, fast running on MABEL. Int. 7. Robot. Res. 32:324

 45
- Ma WL, Kolathaya S, Ambrose ER, Hubicki CM, Ames AD. 2017. Bipedal robotic running with DURUS-2D: bridging the gap between theory and experiment. In *Proceedings of the 20th International Conference on Hybrid Systems: Computation and Control*, pp. 265–74. New York: ACM
- Reher J, Cousineau EA, Hereid A, Hubicki CM, Ames AD. 2016. Realizing dynamic and efficient bipedal locomotion on the humanoid robot DURUS. In 2016 IEEE International Conference on Robotics and Automation, pp. 1794–801. Piscataway, NJ: IEEE
- Reher J, Hereid A, Kolathaya S, Hubicki CM, Ames AD. 2016. Algorithmic foundations of realizing multi-contact locomotion on the humanoid robot DURUS. In *Algorithmic Foundations of Robotics XII*, ed. K Goldberg, P Abbeel, K Bekris, L Miller, pp. 401–15. Cham, Switz.: Springer
- Hereid A, Ames AD. 2017. FROST: Fast Robot Optimization and Simulation Toolkit. In 2017 IEEE/RSJ International Conference on Intelligent Robots and Systems, pp. 719–26. Piscataway, NJ: IEEE
- 23. Featherstone R. 2014. Rigid Body Dynamics Algorithms. New York: Springer
- 24. Pfeiffer F, Glocker C. 1996. Multibody Dynamics with Unilateral Contacts. New York: Wiley & Sons
- Murray RM, Li Z, Sastry SS. 1994. A Mathematical Introduction to Robotic Manipulation. Boca Raton, FL: CRC
- Grizzle JW, Chevallereau C, Sinnet RW, Ames AD. 2014. Models, feedback control, and open problems of 3D bipedal robotic walking. Automatica 50:1955–88
- Vukobratović M, Frank AA, Juricic D. 1970. On the stability of biped locomotion. *IEEE Trans. Biomed. Eng.* BME-17:25–36
- Arakawa T, Fukuda T. 1997. Natural motion generation of biped locomotion robot using hierarchical trajectory generation method consisting of GA, EP layers. In *Proceedings of the International Conference* on Robotics and Automation, Vol. 1, pp. 211–16. Piscataway, NJ: IEEE
- Shih CL, Li Y, Churng S, Lee TT, Gruver WA. 1990. Trajectory synthesis and physical admissibility
 for a biped robot during the single-support phase. In *Proceedings of the IEEE International Conference on Robotics and Automation*, pp. 1646–52. Piscataway, NJ: IEEE
- Yamaguchi Ji, Takanishi A, Kato I. 1993. Development of a biped walking robot compensating for threeaxis moment by trunk motion. J. Robot. Soc. Jpn. 11:581–86
- 31. Sardain P, Bessonnet G. 2004. Forces acting on a biped robot. Center of pressure–zero moment point. IEEE Trans. Syst. Man Cybernet. A 34:630–37
- 32. Hirukawa H, Hattori S, Harada K, Kajita S, Kaneko K, et al. 2006. A universal stability criterion of the foot contact of legged robots adios ZMP. In *Proceedings of the 2006 IEEE International Conference on Robotics and Automation*, pp. 1976–83. Piscataway, NJ: IEEE
- 33. Kajita S, Matsumoto O, Saigo M. 2001. Real-time 3D walking pattern generation for a biped robot with telescopic legs. In *Proceedings of the 2001 IEEE International Conference on Robotics and Automation*, Vol. 3, pp. 2299–306. Piscataway, NJ: IEEE
- 34. Kajita S, Kanehiro F, Kaneko K, Fujiwara K, Harada K, et al. 2003. Biped walking pattern generation by using preview control of zero-moment point. In *Proceedings of the 2003 IEEE International Conference on Robotics and Automation*, Vol. 2, pp. 1620–26. Piscataway, NJ: IEEE

- 35. Pfeiffer F, Loffler K, Gienger M. 2002. The concept of jogging Johnnie. In *Proceedings of the 2002 IEEE International Conference on Robotics and Automation*, Vol. 3, pp. 3129–35. Piscataway, NJ: IEEE
- 36. Pratt J, Carff J, Drakunov S, Goswami A. 2006. Capture point: a step toward humanoid push recovery. In 2006 6th IEEE-RAS International Conference on Humanoid Robots, pp. 200–7. Piscataway, NJ: IEEE
- Hof AL. 2008. The extrapolated center of mass concept suggests a simple control of balance in walking. Hum. Mov. Sci. 27:112–25
- Koolen T, De Boer T, Rebula J, Goswami A, Pratt J. 2012. Capturability-based analysis and control of legged locomotion, part 1: theory and application to three simple gait models. *Int. J. Robot. Res.* 31:1094– 113
- Johnson M, Shrewsbury B, Bertrand S, Wu T, Duran D, et al. 2015. Team IHMC's lessons learned from the DARPA robotics challenge trials. 7. Field Robot. 32:192–208
- 40. Kuindersma S, Deits R, Fallon M, Valenzuela A, Dai H, et al. 2016. Optimization-based locomotion planning, estimation, and control design for the Atlas humanoid robot. *Auton. Robots* 40:429–55
- 41. DeDonato M, Dimitrov V, Du R, Giovacchini R, Knoedler K, et al. 2015. Human-in-the-loop control of a humanoid robot for disaster response: a report from the DARPA robotics challenge trials. *J. Field Robot.* 32:275–92
- 42. Pratt JE, Drakunov SV. 2007. Derivation and application of a conserved orbital energy for the inverted pendulum bipedal walking model. In *Proceedings of the 2007 IEEE International Conference on Robotics and Automation*, pp. 4653–60. Piscataway, NJ: IEEE
- Park JH, Kim KD. 1998. Biped robot walking using gravity-compensated inverted pendulum mode and computed torque control. In *Proceedings of the 1998 IEEE International Conference on Robotics and Automation*, Vol. 4, pp. 3528–33. Piscataway, NJ: IEEE
- Stephens B. 2011. Push recovery control for force-controlled humanoid robots. PhD Thesis, Carnegie Mellon Univ., Pittsburgh, PA
- 45. Pratt J, Koolen T, De Boer T, Rebula J, Cotton S, et al. 2012. Capturability-based analysis and control of legged locomotion, part 2: application to M2V2, a lower-body humanoid. *Int. 7. Robot. Res.* 31:1117–33
- 46. Hof A, Gazendam M, Sinke W. 2005. The condition for dynamic stability. 7. Biomech. 38:1-8
- Hyon SH, Hale JG, Cheng G. 2007. Full-body compliant human-humanoid interaction: balancing in the presence of unknown external forces. *IEEE Trans. Robot.* 23:884–98
- 48. Stephens B. 2007. Humanoid push recovery. In 2007 7th IEEE-RAS International Conference on Humanoid Robots, pp. 589–95. Piscataway, NJ: IEEE
- 49. Takanishi A, Takeya T, Karaki H, Kato I. 1990. A control method for dynamic biped walking under unknown external force. In EEE International Workshop on Intelligent Robots and Systems: Towards a New Frontier of Applications, pp. 795–801. Piscataway, NJ: IEEE
- Englsberger J, Ott C, Roa MA, Albu-Schäffer A, Hirzinger G. 2011. Bipedal walking control based on capture point dynamics. In 2011 IEEE/RSJ International Conference on Intelligent Robots and Systems, pp. 4420–27. Piscataway, NJ: IEEE
- Takenaka T, Matsumoto T, Yoshiike T. 2009. Real time motion generation and control for biped robot
 1st report: walking gait pattern generation. In 2009 IEEE/RSJ International Conference on Intelligent Robots and Systems, pp. 1084–91. Piscataway, NJ: IEEE
- 52. Sakagami Y, Watanabe R, Aoyama C, Matsunaga S, Higaki N, Fujimura K. 2002. The intelligent ASIMO: system overview and integration. In *IEEE/RSf International Conference on Intelligent Robots and Systems*, Vol. 3, pp. 2478–83. Piscataway, NJ: IEEE
- Geyer H, Seyfarth A, Blickhan R. 2006. Compliant leg behaviour explains basic dynamics of walking and running. Proc. R. Soc. Lond. B 273:2861–67
- 54. Blickhan R. 1989. The spring-mass model for running and hopping. 7. Biomech. 22:1217-27
- 55. Pratt J, Chew CM, Torres A, Dilworth P, Pratt G. 2001. Virtual model control: an intuitive approach for bipedal locomotion. *Int. J. Robot. Res.* 20:129–43
- Ahmadi M, Buehler M. 2006. Controlled passive dynamic running experiments with the ARL-Monopod II. IEEE Trans. Robot. 22:974–86
- Altendorfer R, Koditschek DE, Holmes P. 2004. Stability analysis of legged locomotion models by symmetry-factored return maps. Int. J. Robot. Res. 23:979–99

- Rummel J, Blum Y, Maus HM, Rode C, Seyfarth A. 2010. Stable and robust walking with compliant legs.
 In 2010 IEEE International Conference on Robotics and Automation, pp. 5250–55. Piscataway, NJ: IEEE
- 59. Zeglin G, Brown B. 1998. Control of a bow leg hopping robot. In *Proceedings of the 1998 IEEE International Conference on Robotics and Automation*, Vol. 1, pp. 793–98. Piscataway, NJ: IEEE
- Hobbelen DGE, Wisse M. 2007. Limit cycle walking. In Humanoid Robots: Human-Like Machines, ed. M Hackel, pp. 277–94. London: IntechOpen
- 61. Perko L. 2013. Differential Equations and Dynamical Systems. New York: Springer
- 62. Morris B, Grizzle JW. 2005. A restricted Poincaré map for determining exponentially stable periodic orbits in systems with impulse effects: application to bipedal robots. In *Proceedings of the 44th IEEE Conference on Decision and Control*, pp. 4199–206. Piscataway, NJ: IEEE
- 63. Wendel ED, Ames AD. 2010. Rank properties of Poincaré maps for hybrid systems with applications to bipedal walking. In *Proceedings of the 13th ACM International Conference on Hybrid Systems: Computation and Control*, pp. 151–60. New York: ACM
- Hunter IW, Hollerbach JM, Ballantyne J. 1991. A comparative analysis of actuator technologies for robotics. Robot. Rev. 2:299–342
- Kormushev P, Ugurlu B, Calinon S, Tsagarakis NG, Caldwell DG. 2011. Bipedal walking energy minimization by reinforcement learning with evolving policy parameterization. In 2011 IEEE/RSJ International Conference on Intelligent Robots and Systems, pp. 318–24. Piscataway, NJ: IEEE
- Radford NA, Strawser P, Hambuchen K, Mehling JS, Verdeyen WK, et al. 2015. Valkyrie: NASA's first bipedal humanoid robot. 7. Field Robot. 32:397

 –419
- Park HW, Sreenath K, Hurst JW, Grizzle JW. 2011. Identification of a bipedal robot with a compliant drivetrain. IEEE Control Syst. 31:63–88
- 68. Grimes JA, Hurst JW. 2012. The design of ATRIAS 1.0: a unique monopod, hopping robot. In Adaptive Mobile Robotics: Proceedings of the 15th International Conference on Climbing and Walking Robots and the Support Technologies for Mobile Machines, ed. AKM Azad, NJ Cowan, MO Tokhi, GS Virk, RD Eastman, pp. 548–54. Singapore: World Sci.
- 69. Rezazadeh S, Hubicki C, Jones M, Peekema A, Van Why J, et al. 2015. Spring-mass walking with ATRIAS in 3D: robust gait control spanning zero to 4.3 kph on a heavily underactuated bipedal robot. In *Proceedings of the ASME 2015 Dynamic Systems and Control Conference*, pap. DSCC2015-9899. New York: Am. Soc. Mech. Eng.
- 70. Abate AM. 2018. Mechanical design for robot locomotion. PhD Thesis, Ore. State Univ., Corvallis
- Ahmadi M, Buehler M. 1999. The ARL Monopod II running robot: control and energetics. In Proceedings
 of the 1999 IEEE International Conference on Robotics and Automation, Vol. 3, pp. 1689–94. Piscataway, NJ:
 IEEE
- 72. Brown B, Zeglin G. 1998. The bow leg hopping robot. In *Proceedings of the 1998 IEEE International Conference on Robotics and Automation*, Vol. 1, pp. 781–86. Piscataway, NJ: IEEE
- Hyon SH, Mita T. 2002. Development of a biologically inspired hopping robot "Kenken". In Proceedings of the 2002 IEEE International Conference on Robotics and Automation, Vol. 4, pp. 3984–91. Piscataway, NI: IEEE
- McGeer T. 1990. Passive walking with knees. In Proceedings of the 1990 IEEE International Conference on Robotics and Automation, pp. 1640–45. Piscataway, NJ: IEEE
- Collins SH, Wisse M, Ruina A. 2001. A three-dimensional passive-dynamic walking robot with two legs and knees. Int. J. Robot. Res. 20:607–15
- Collins SH, Ruina A. 2005. A bipedal walking robot with efficient and human-like gait. In Proceedings of the 2005 IEEE International Conference on Robotics and Automation, pp. 1983–88. Piscataway, NJ: IEEE
- Bhounsule P, Ruina A. 2009. Cornell Ranger: energy-optimal control. Paper presented at Dynamic Walking 2009, Vancouver, Can., June 7–11
- Tedrake R, Zhang TW, Seung HS. 2004. Stochastic policy gradient reinforcement learning on a simple 3D biped. In 2004 IEEE/RSJ International Conference on Intelligent Robots and Systems, Vol. 3, pp. 2849–54. Piscataway, NJ: IEEE
- Tedrake R, Zhang TW, Fong M, Seung HS. 2004. Actuating a simple 3D passive dynamic walker. In Proceedings of the 2004 IEEE International Conference on Robotics and Automation, Vol. 5, pp. 4656–61. Piscataway, NJ: IEEE

- Anderson SO, Wisse M, Atkeson CG, Hodgins JK, Zeglin G, Moyer B. 2005. Powered bipeds based on passive dynamic principles. In 5th IEEE-RAS International Conference on Humanoid Robots, pp. 110–16. Piscataway, NJ: IEEE
- 81. Wisse M, Van der Linde RQ. 2007. Delft Pneumatic Bipeds. Berlin: Springer
- 82. Spong MW, Bullo F. 2005. Controlled symmetries and passive walking. *IEEE Trans. Autom. Control* 50:1025–31
- 83. Ames AD, Gregg RD, Spong MW. 2007. A geometric approach to three-dimensional hipped bipedal robotic walking. In 2007 46th IEEE Conference on Decision and Control, pp. 5123–30. Piscataway, NJ: IEEE
- Reher J, Csomay-Shanklin N, Christensen DL, Bristow B, Ames AD, Smoot L. 2020. Passive dynamic balancing and walking in actuated environments. In 2020 IEEE International Conference on Robotics and Automation, pp. 9775–81. Piscataway, NJ: IEEE
- Ames AD, Vasudevan R, Bajcsy R. 2011. Human-data based cost of bipedal robotic walking. In Proceedings
 of the 14th International Conference on Hybrid Systems: Computation and Control, pp. 153–62. New York:
 ACM
- Ames AD. 2012. First steps toward automatically generating bipedal robotic walking from human data.
 In Robot Motion and Control 2011, ed. K Kozlowski, pp. 89–116. London: Springer
- 87. Pfeiffer F, Glocker C. 1996. Multibody Dynamics with Unilateral Contacts. New York: Wiley & Sons
- Hurmuzlu Y, Marghitu DB. 1994. Rigid body collisions of planar kinematic chains with multiple contact points. Int. 7. Robot. Res. 13:82–92
- Or Y. 2014. Painlevé's paradox and dynamic jamming in simple models of passive dynamic walking. Regul. Chaotic Dyn. 19:64–80
- Liu C, Zhao Z, Brogliato B. 2008. Frictionless multiple impacts in multibody systems. I. Theoretical framework. Proc. R. Soc. A 464:3193–211
- Or Y, Ames AD. 2010. Stability and completion of Zeno equilibria in Lagrangian hybrid systems. IEEE Trans. Autom. Control 56:1322–36
- 92. Lamperski A, Ames AD. 2012. Lyapunov theory for Zeno stability. IEEE Trans. Autom. Control 58:100-12
- Ames AD. 2011. Characterizing knee-bounce in bipedal robotic walking: a Zeno behavior approach. In Proceedings of the 14th International Conference on Hybrid Systems: Computation and Control, pp. 163–72. New York: ACM
- Marton L, Lantos B. 2007. Modeling, identification, and compensation of stick-slip friction. IEEE Trans. Ind. Electron. 54:511–21
- 95. Ma WL, Or Y, Ames AD. 2019. Dynamic walking on slippery surfaces: demonstrating stable bipedal gaits with planned ground slippage. In 2019 International Conference on Robotics and Automation, pp. 3705–11. Piscataway, NJ: IEEE
- Goswami A, Thuilot B, Espiau B. 1998. A study of the passive gait of a compass-like biped robot: symmetry and chaos. Int. J. Robot. Res. 17:1282–301
- 97. Morris B, Grizzle JW. 2009. Hybrid invariant manifolds in systems with impulse effects with application to periodic locomotion in bipedal robots. *IEEE Trans. Autom. Control* 54:1751–64
- 98. Grizzle JW, Abba G, Plestan F. 2001. Asymptotically stable walking for biped robots: analysis via systems with impulse effects. *IEEE Trans. Autom. Control* 46:51–64
- Sinnet RW, Ames AD. 2009. 2D bipedal walking with knees and feet: a hybrid control approach. In Proceedings of the 48th IEEE Conference on Decision and Control Held Jointly with 2009 28th Chinese Control Conference, pp. 3200–7. Piscataway, NJ: IEEE
- Reher J, Ma WL, Ames AD. 2019. Dynamic walking with compliance on a Cassie bipedal robot. In 2019 18th European Control Conference, pp. 2589–95. Piscataway, NJ: IEEE
- 101. Sastry SS. 2013. Nonlinear Systems: Analysis, Stability, and Control. New York: Springer
- 102. Isidori A. 1997. Nonlinear Control Systems. London: Springer
- 103. Ames AD. 2014. Human-inspired control of bipedal walking robots. *IEEE Trans. Autom. Control* 59:1115–
- Chevallereau C, Abba G, Aoustin Y, Plestan F, Westervelt E, et al. 2003. Rabbit: a testbed for advanced control theory. IEEE Control Syst. Mag. 23(5):57–79
- Grizzle JW, Hurst J, Morris B, Park HW, Sreenath K. 2009. MABEL, a new robotic bipedal walker and runner. In 2009 American Control Conference, pp. 2030–36. Piscataway, NJ: IEEE

- 106. Yadukumar SN, Pasupuleti M, Ames AD. 2013. From formal methods to algorithmic implementation of human inspired control on bipedal robots. In *Algorithmic Foundations of Robotics X*, ed. E Frazzoli, T Lozano-Perez, N Roy, D Rus, pp. 511–26. Berlin: Springer
- Hamed KA, Grizzle JW. 2013. Event-based stabilization of periodic orbits for underactuated 3-D bipedal robots with left-right symmetry. IEEE Trans. Robot. 30:365–81
- Ramezani A, Hurst JW, Akbari Hamed K, Grizzle JW. 2014. Performance analysis and feedback control of ATRIAS, a three-dimensional bipedal robot. J. Dyn. Syst. Meas. Control 136:021012
- Zhao HH, Ma WL, Zeagler MB, Ames AD. 2014. Human-inspired multi-contact locomotion with AM-BER2. In 2014 ACM/IEEE International Conference on Cyber-Physical Systems, pp. 199–210. Piscataway, NI: IEEE
- Ambrose E, Ma WL, Hubicki C, Ames AD. 2017. Toward benchmarking locomotion economy across design configurations on the modular robot: AMBER-3M. In 2017 IEEE Conference on Control Technology and Applications, pp. 1270–76. Piscataway, NJ: IEEE
- 111. Ames AD, Cousineau EA, Powell MJ. 2012. Dynamically stable bipedal robotic walking with NAO via human-inspired hybrid zero dynamics. In Proceedings of the 15th ACM International Conference on Hybrid Systems: Computation and Control, pp. 135–44. New York: ACM
- 112. Buss BG, Ramezani A, Hamed KA, Griffin BA, Galloway KS, Grizzle JW. 2014. Preliminary walking experiments with underactuated 3D bipedal robot MARLO. In 2014 IEEE/RSJ International Conference on Intelligent Robots and Systems, pp. 2529–36. Piscataway, NJ: IEEE
- Zhao H, Horn J, Reher J, Paredes V, Ames AD. 2016. Multicontact locomotion on transfemoral prostheses via hybrid system models and optimization-based control. *IEEE Trans. Autom. Sci. Eng.* 13:502–13
- Zhao H, Horn J, Reher J, Paredes V, Ames AD. 2017. First steps toward translating robotic walking to prostheses: a nonlinear optimization based control approach. *Auton. Robots* 41:725–42
- 115. Zhao H, Ambrose E, Ames AD. 2017. Preliminary results on energy efficient 3D prosthetic walking with a powered compliant transfemoral prosthesis. In 2017 IEEE International Conference on Robotics and Automation, pp. 1140–47. Piscataway, NJ: IEEE
- Harib O, Hereid A, Agrawal A, Gurriet T, Finet S, et al. 2018. Feedback control of an exoskeleton for paraplegics: toward robustly stable, hands-free dynamic walking. IEEE Control Syst. Mag. 38(6):61–87
- 117. Gurriet T, Finet S, Boeris G, Duburcq A, Hereid A, et al. 2018. Towards restoring locomotion for paraplegics: realizing dynamically stable walking on exoskeletons. In 2018 IEEE International Conference on Robotics and Automation, pp. 2804–11. Piscataway, NJ: IEEE
- Poulakakis I. 2009. Stabilizing monopedal robot running: reduction-by-feedback and compliant bybrid zero dynamics. PhD Thesis, Univ. Mich., Ann Arbor
- Gong Y, Hartley R, Da X, Hereid A, Harib O, et al. 2019. Feedback control of a Cassie bipedal robot: walking, standing, and riding a Segway. In 2019 American Control Conference, pp. 4559

 –66. Piscataway, NJ: IEEE
- Stumpf A, Kohlbrecher S, Conner DC, von Stryk O. 2016. Open source integrated 3D footstep planning framework for humanoid robots. In 2016 IEEE-RAS 16th International Conference on Humanoid Robots, pp. 938–45. Piscataway, NJ: IEEE
- 121. Nishiwaki K, Kagami S. 2009. Online walking control system for humanoids with short cycle pattern generation. *Int. J. Robot. Res.* 28:729–42
- 122. Wieber PB. 2006. Trajectory free linear model predictive control for stable walking in the presence of strong perturbations. In 2006 6th IEEE-RAS International Conference on Humanoid Robots, pp. 137–42. Piscataway, NJ: IEEE
- Stephens BJ, Atkeson CG. 2010. Push recovery by stepping for humanoid robots with force controlled joints. In 2010 10th IEEE-RAS International Conference on Humanoid Robots, pp. 52–59. Piscataway, NJ: IEEE
- Wieber PB. 2008. Viability and predictive control for safe locomotion. In 2008 IEEE/RSJ International Conference on Intelligent Robots and Systems, pp. 1103–8. Piscataway, NJ: IEEE
- 125. Huang Q, Kajita S, Koyachi N, Kaneko K, Yokoi K, et al. 1999. A high stability, smooth walking pattern for a biped robot. In *Proceedings of the 1999 IEEE International Conference on Robotics and Automation*, Vol. 1, pp. 65–71. Piscataway, NJ: IEEE

- 126. Kajita S, Kanehiro F, Kaneko K, Fujiwara K, Harada K, et al. 2003. Biped walking pattern generation by using preview control of zero-moment point. In 2003 IEEE International Conference on Robotics and Automation, Vol. 2, pp. 1620-26. Piscataway, NJ: IEEE
- 127. Nagasaka K, Inoue H, Inaba M. 1999. Dynamic walking pattern generation for a humanoid robot based on optimal gradient method. In IEEE SMC'99 Conference Proceedings: 1999 IEEE International Conference on Systems, Man, and Cybernetics, Vol. 6, pp. 908-13. Piscataway, NJ: IEEE
- 128. Khatib O. 1987. A unified approach for motion and force control of robot manipulators: the operational space formulation. IEEE 7. Robot. Autom. 3:43-53
- 129. Hebert P, Bajracharya M, Ma J, Hudson N, Aydemir A, et al. 2015. Mobile manipulation and mobility as manipulation—design and algorithms of RoboSimian. J. Field Robot. 32:255-74
- 130. Zucker M, Joo S, Grey MX, Rasmussen C, Huang E, et al. 2015. A general-purpose system for teleoperation of the DRC-HUBO humanoid robot. J. Field Robot. 32:336-51
- 131. Chow C, Jacobson D. 1971. Studies of human locomotion via optimal programming. Math. Biosci. 10:239-306
- 132. Channon P, Hopkins S, Pham D. 1992. Derivation of optimal walking motions for a bipedal walking robot. *Robotica* 10:165-72
- 133. Mombaur K. 2009. Using optimization to create self-stable human-like running. Robotica 27:321–30
- 134. Mombaur KD, Bock HG, Schlöder JP, Longman RW. 2005. Open-loop stable solutions of periodic optimal control problems in robotics. Z. Angew. Math. Mech. 85:499-515
- 135. Dai H, Valenzuela A, Tedrake R. 2014. Whole-body motion planning with centroidal dynamics and full kinematics. In 2014 IEEE-RAS International Conference on Humanoid Robots, pp. 295-302. Piscataway, NJ:
- 136. Posa M, Kuindersma S, Tedrake R. 2016. Optimization and stabilization of trajectories for constrained dynamical systems. In 2016 IEEE International Conference on Robotics and Automation, pp. 1366-73. Piscataway, NJ: IEEE
- 137. Herzog A, Rotella N, Schaal S, Righetti L. 2015. Trajectory generation for multi-contact momentum control. In 2015 IEEE-RAS 15th International Conference on Humanoid Robots, pp. 874–80. Piscataway, NJ:
- 138. Posa M, Cantu C, Tedrake R. 2014. A direct method for trajectory optimization of rigid bodies through contact. Int. 7. Robot. Res. 33:69-81
- 139. Moreau JJ. 1966. Quadratic programming in mechanics: dynamics of one-sided constraints. SIAM J. Control 4:153-58
- 140. Denk J, Schmidt G. 2001. Synthesis of a walking primitive database for a humanoid robot using optimal control techniques. In Proceedings of the IEEE-RAS International Conference on Humanoid Robots, pp. 319-26. Piscataway, NJ: IEEE
- 141. Hereid A, Cousineau EA, Hubicki CM, Ames AD. 2016. 3D dynamic walking with underactuated humanoid robots: a direct collocation framework for optimizing hybrid zero dynamics. In 2016 IEEE International Conference on Robotics and Automation, pp. 1447–54. Piscataway, NJ: IEEE
- 142. Hereid A, Hubicki CM, Cousineau EA, Hurst JW, Ames AD. 2015. Hybrid zero dynamics based multiple shooting optimization with applications to robotic walking. In 2015 IEEE International Conference on Robotics and Automation, pp. 5734-40. Piscataway, NJ: IEEE
- 143. Hereid A, Hubicki CM, Cousineau EA, Ames AD. 2018. Dynamic humanoid locomotion: a scalable formulation for HZD gait optimization. IEEE Trans. Robot. 34:370-87
- 144. Da X, Harib O, Hartley R, Griffin B, Grizzle JW. 2016. From 2D design of underactuated bipedal gaits to 3D implementation: walking with speed tracking. IEEE Access 4:3469-78
- 145. Da X, Hartley R, Grizzle JW. 2017. Supervised learning for stabilizing underactuated bipedal robot locomotion, with outdoor experiments on the wave field. In 2017 IEEE International Conference on Robotics and Automation, pp. 3476-83. Piscataway, NJ: IEEE
- 146. Ziegler JG, Nichols NB. 1942. Optimum settings for automatic controllers. Trans. ASME 64:759-68
- 147. Kolathaya S, Hereid A, Ames AD. 2016. Time dependent control Lyapunov functions and hybrid zero dynamics for stable robotic locomotion. In 2016 American Control Conference, pp. 3916–21. Piscataway, NJ: IEEE

- Westervelt ER, Buche G, Grizzle JW. 2004. Experimental validation of a framework for the design of controllers that induce stable walking in planar bipeds. Int. J. Robot. Res. 23:559–82
- 149. Kajita S, Kanehiro F, Kaneko K, Fujiwara K, Harada K, et al. 2003. Resolved momentum control: humanoid motion planning based on the linear and angular momentum. In *Proceedings of the 2003 IEEE/RSJ International Conference on Intelligent Robots and Systems*, Vol. 2, pp. 1644–50. Piscataway, NJ: IEEE
- Popovic M, Hofmann A, Herr H. 2004. Zero spin angular momentum control: definition and applicability. In 4th IEEE/RAS International Conference on Humanoid Robots, Vol. 1, pp. 478–93. Piscataway, NJ: IFFF
- 151. Lee SH, Goswami A. 2010. Ground reaction force control at each foot: a momentum-based humanoid balance controller for non-level and non-stationary ground. In 2010 IEEE/RSJ International Conference on Intelligent Robots and Systems, pp. 3157–62. Piscataway, NJ: IEEE
- 152. Koolen T, Bertrand S, Thomas G, De Boer T, Wu T, et al. 2016. Design of a momentum-based control framework and application to the humanoid robot Atlas. *Int. 7. Humanoid Robot.* 13:1650007
- 153. Fujimoto Y, Kawamura A. 1996. Proposal of biped walking control based on robust hybrid position/ force control. In *Proceedings of the IEEE International Conference on Robotics and Automation*, Vol. 3, pp. 2724–30. Piscataway, NJ: IEEE
- Saab L, Ramos OE, Keith F, Mansard N, Soueres P, Fourquet JY. 2013. Dynamic whole-body motion generation under rigid contacts and other unilateral constraints. IEEE Trans. Robot. 29:346–62
- Tzafestas S, Raibert M, Tzafestas C. 1996. Robust sliding-mode control applied to a 5-link biped robot.
 Intell. Robot. Syst. 15:67–133
- 156. Ames AD, Powell M. 2013. Towards the unification of locomotion and manipulation through control Lyapunov functions and quadratic programs. In *Control of Cyber-Physical Systems*, ed. D Tarrag, pp. 219–40. Heidelberg, Ger.: Springer
- 157. Sentis L. 2007. Synthesis and control of whole-body behaviors in humanoid systems. PhD Thesis, Stanford Univ., Stanford, CA
- 158. Aghili F. 2005. A unified approach for inverse and direct dynamics of constrained multibody systems based on linear projection operator: applications to control and simulation. *IEEE Trans. Robot.* 21:834–49
- Mistry M, Buchli J, Schaal S. 2010. Inverse dynamics control of floating base systems using orthogonal decomposition. In 2010 IEEE International Conference on Robotics and Automation, pp. 3406–12. Piscataway, NJ: IEEE
- 160. Apgar T, Clary P, Green K, Fern A, Hurst JW. 2018. Fast online trajectory optimization for the bipedal robot Cassie. In *Robotics: Science and Systems XIV*, ed. H Kress-Gazit, S Srinivasa, T Howard, N Atanasov, pap. 54. N.p.: Robot. Sci. Syst. Found.
- Feng S, Whitman E, Xinjilefu X, Atkeson CG. 2015. Optimization-based full body control for the DARPA robotics challenge. J. Field Robot. 32:293–312
- 162. Herzog A, Rotella N, Mason S, Grimminger F, Schaal S, Righetti L. 2016. Momentum control with hierarchical inverse dynamics on a torque-controlled humanoid. *Auton. Robots* 40:473–91
- Ames AD, Galloway K, Grizzle JW. 2012. Control Lyapunov functions and hybrid zero dynamics. In 2012 IEEE 51st IEEE Conference on Decision and Control, pp. 6837

 –42. Piscataway, NJ: IEEE
- Galloway K, Sreenath K, Ames AD, Grizzle JW. 2015. Torque saturation in bipedal robotic walking through control Lyapunov function-based quadratic programs. IEEE Access 3:323–32
- 165. Cousineau E, Ames AD. 2015. Realizing underactuated bipedal walking with torque controllers via the ideal model resolved motion method. In 2015 IEEE International Conference on Robotics and Automation, pp. 5747–53. Piscataway, NJ: IEEE
- Nguyen Q, Sreenath K. 2020. Optimal robust safety-critical control for dynamic robotics. arXiv:2005.07284 [cs.RO]
- 167. Reher J, Kann C, Ames AD. 2020. An inverse dynamics approach to control Lyapunov functions. In 2020 American Control Conference, pp. 2444–51. Piscataway, NJ: IEEE
- Ames AD, Holley J. 2014. Quadratic program based nonlinear embedded control of series elastic actuators. In 53rd IEEE Conference on Decision and Control, pp. 6291–98. Piscataway, NJ: IEEE

- Hereid A, Powell MJ, Ames AD. 2014. Embedding of SLIP dynamics on underactuated bipedal robots through multi-objective quadratic program based control. In 2014 IEEE 53rd Annual Conference on Decision and Control, pp. 2950–57. Piscataway, NJ: IEEE
- 170. Xiong X, Ames AD. 2018. Coupling reduced order models via feedback control for 3D underactuated bipedal robotic walking. In 2018 IEEE-RAS 18th International Conference on Humanoid Robots. Piscataway, NJ: IEEE. https://doi.org/10.1109/HUMANOIDS.2018.8625066
- 171. Xiong X, Ames AD. 2018. Bipedal hopping: reduced-order model embedding via optimization-based control. In 2018 IEEE/RSJ International Conference on Intelligent Robots and Systems, pp. 3821–28. Piscat-away, NJ: IEEE
- Wieber PB, Chevallereau C. 2006. Online adaptation of reference trajectories for the control of walking systems. Robot. Auton. Syst. 54:559–66
- 173. Chevallereau C, Westervelt E, Grizzle J. 2005. Asymptotically stable running for a five-link, four-actuator, planar bipedal robot. *Int. J. Robot. Res.* 24:431–64
- 174. Powell MJ, Hereid A, Ames AD. 2013. Speed regulation in 3D robotic walking through motion transitions between human-inspired partial hybrid zero dynamics. In 2013 IEEE International Conference on Robotics and Automation, pp. 4803–10. Piscataway, NJ: IEEE
- 175. Rezazadeh S, Hubicki CM, Jones M, Peekema A, Van Why J, et al. 2015. Spring-mass walking with ATRIAS in 3D: robust gait control spanning zero to 4.3 kph on a heavily underactuated bipedal robot. In *Proceedings of the ASME 2015 Dynamic Systems and Control Conference*, pap. DSCC2015-9899. New York: Am. Soc. Mech. Eng.
- Griffin B, Grizzle J. 2015. Nonholonomic virtual constraints for dynamic walking. In 2015 54th IEEE Conference on Decision and Control, pp. 4053–60. Piscataway, NJ: IEEE
- 177. Nguyen Q, Hereid A, Grizzle JW, Ames AD, Sreenath K. 2016. 3D dynamic walking on stepping stones with control barrier functions. In 2016 IEEE 55th Conference on Decision and Control, pp. 827–34. Piscataway, NJ: IEEE
- 178. Ames AD, Tabuada P, Jones A, Ma WL, Rungger M, et al. 2017. First steps toward formal controller synthesis for bipedal robots with experimental implementation. *Nonlinear Anal. Hybrid Syst.* 25:155–73
- Ames AD, Xu X, Grizzle JW, Tabuada P. 2016. Control barrier function based quadratic programs for safety critical systems. *IEEE Trans. Autom. Control* 62:3861–76
- 180. Hereid A, Kolathaya S, Ames AD. 2016. Online optimal gait generation for bipedal walking robots using Legendre pseudospectral optimization. In 2016 IEEE 55th Conference on Decision and Control, pp. 6173-79. Piscataway, NJ: IEEE



Annual Review of Control, Robotics, and Autonomous Systems

Volume 4, 2021

Contents

What Is Robotics? Why Do We Need It and How Can We Get It? Daniel E. Koditschek	
The Role of Physics-Based Simulators in Robotics C. Karen Liu and Dan Negrut	35
Koopman Operators for Estimation and Control of Dynamical Systems Samuel E. Otto and Clarence W. Rowley	59
Optimal Transport in Systems and Control Yongxin Chen, Tryphon T. Georgiou, and Michele Pavon	89
Communication-Aware Robotics: Exploiting Motion for Communication Arjun Muralidbaran and Yasamin Mostofi	11:
Factor Graphs: Exploiting Structure in Robotics Frank Dellaert	14
Brain–Machine Interfaces: Closed-Loop Control in an Adaptive System Ethan Sorrell, Michael E. Rule, and Timothy O'Leary	167
Noninvasive Brain–Machine Interfaces for Robotic Devices Luca Tonin and José del R. Millán	191
Advances in Inference and Representation for Simultaneous Localization and Mapping David M. Rosen, Kevin J. Doherty, Antonio Terán Espinoza, and John J. Leonard	21:
Markov Chain—Based Stochastic Strategies for Robotic Surveillance Xiaoming Duan and Francesco Bullo	243
Integrated Task and Motion Planning Caelan Reed Garrett, Rohan Chitnis, Rachel Holladay, Beomjoon Kim, Tom Silver, Leslie Pack Kaelbling, and Tomás Lozano-Pérez	265
Asymptotically Optimal Sampling-Based Motion Planning Methods Jonathan D. Gammell and Marlin P. Strub	295

Scalable Control of Positive Systems Anders Rantzer and Maria Elena Valcher	319
Optimal Quantum Control Theory M.R. James	343
Set Propagation Techniques for Reachability Analysis Matthias Althoff, Goran Frehse, and Antoine Girard	369
Control and Optimization of Air Traffic Networks Karthik Gopalakrishnan and Hamsa Balakrishnan	397
Model Reduction Methods for Complex Network Systems X. Cheng and J.M.A. Scherpen	425
Analysis and Interventions in Large Network Games Francesca Parise and Asuman Ozdaglar	455
Animal-in-the-Loop: Using Interactive Robotic Conspecifics to Study Social Behavior in Animal Groups Tim Landgraf, Gregor H.W. Gebhardt, David Bierbach, Pawel Romanczuk, Lea Musiolek, Verena V. Hafner, and Jens Krause	487
Motion Control in Magnetic Microrobotics: From Individual and Multiple Robots to Swarms Lidong Yang and Li Zhang	509
Dynamic Walking: Toward Agile and Efficient Bipedal Robots *Jenna Reher and Aaron D. Ames	535
Mechanisms for Robotic Grasping and Manipulation Vincent Babin and Clément Gosselin	573
Current Solutions and Future Trends for Robotic Prosthetic Hands Vincent Mendez, Francesco Iberite, Solaiman Shokur, and Silvestro Micera	595
Electronic Skins for Healthcare Monitoring and Smart Prostheses Haotian Chen, Laurent Dejace, and Stéphanie P. Lacour	629
Autonomy in Surgical Robotics Aleks Attanasio, Bruno Scaglioni, Elena De Momi, Paolo Fiorini, and Pietro Valdastri	
The Use of Robots to Respond to Nuclear Accidents: Applying the Lessons of the Past to the Fukushima Daiichi Nuclear Power Station <i>Yasuyoshi Yokokohji</i>	681

Errata

An online log of corrections to *Annual Review of Control, Robotics, and Autonomous Systems* articles may be found at http://www.annualreviews.org/errata/control